Dimethyl fumarate and monomethyl fumarate attenuate oxidative stress and mitochondrial alterations leading to oxiapoptophagy in 158N murine oligodendrocytes treated with 7β-hydroxycholesterol

Randa Sghaier, Thomas Nury, Valerio Leoni, Claudio Caccia, Jean-Paul Pais de Barros, Ameur Cherif, Anne Vejux, Thibault Moreau, Khalifa Limem, Mohammad Samadi, et al.

Dimethyl fumarate and monomethyl fumarate attenuate oxidative stress and mitochondrial alterations leading to oxiapoptophagy in 158N murine oligodendrocytes treated with 7β-hydroxycholesterol

Randa SGHAIER, [1,2,3,4] Thomas NURY, [1] Valerio LEONI, [5] Claudio CACCIA, [6] Jean-Paul PAIS DE BARROS, [7] Ameur CHERIF, [4] Anne VEJUX, [1] Thibault MOREAU, [1,8] , Khalifa Limem, [2] Mohammad SAMADI, [9] John J. MACKRILL, [10] Ahmed Slaheddine MASMOUDI, [4] Gérard LIZARD,[1*] Amira ZARROUK [2,3 *]

[1] *Univ. Bourgogne Franche-Comté, Team 'Biochemistry of the Peroxisome, Inflammation and Lipid Metabolism' EA 7270 / Inserm, Dijon, France*

[2] *Univ. Sousse, Laboratory of Biochemistry, Faculty of Medicine, Tunisia*

[3] *Univ. Monastir, Faculty of Medicine, LR12ES05, Lab-NAFS 'Nutrition - Functional Food & Vascular Health', Monastir, & Univ. Sousse, Faculty of Medicine, Sousse, Tunisia*

[4] *Univ. Manouba, Laboratory of Biotechnology and Valorisation of Bio-Géo Ressources (LR11ES31), Higher Institute of Biotechnology, Sidi Thabet, Tunisia*

[5] *Laboratory of Clinical Chemistry, Hospital of Varese, ASST-Settelaghi, Varese, Italy*

[6] *Unit of Medical Genetics and Neurogenetics, IRCCS Carlo Besta, Milano, Italy*

[7] *Univ. Bourgogne, Lipidomic platform, Dijon, France*

[8] *Univ. Hospital, Department of Neurology, Dijon, France*

[9] *LCPMC-A2, ICPM, Dept of Chemistry, Univ. Lorraine, Metz Technopôle, Metz, France*

[10] Department of Physiology, Biosciences Institute, University College Cork, Cork, Ireland

Correspondence: Dr Amira ZARROUK (zarroukamira@gmail.com) and Dr Gérard LIZARD (gerard.lizard@u-bourgogne.fr). Dr ZARROUK and Dr LIZARD equally contributed to the design and the supervision of the study.

Abstract

Oxidative stress and mitochondrial dysfunction contribute to the pathogenesis of neurodegenerative diseases and favor lipid peroxidation, leading to increased levels of 7β-hydroxycholesterol (7β-OHC) which induces oxiapoptophagy (OXIdative stress, APOPTOsis, autoPHAGY). The cytoprotective effects of dimethylfumarate (DMF), used in the treatment of relapsing remitting multiple sclerosis and of monomethylfumarate (MMF), its main metabolite, were evaluated on murine oligodendrocytes 158N exposed to 7β-OHC (50 μM, 24 h) with or without DMF or MMF (25 μM). The activity of 7β-OHC in the presence or absence DMF or MMF was evaluated on several parameters: cell adhesion; plasma membrane integrity measured with propidium iodide (PI), trypan blue and fluoresceine diacetate (FDA) assays; LDH activity; antioxidant enzyme activities (superoxide dismutase (SOD), catalase (CAT) and glutathione peroxidase (GPx)); generation of lipid peroxidation products (malondialdehyde (MDA), conjugated dienes (CDs)) and protein oxidation products (carbonylated proteins (CPs)); reactive oxygen species (ROS) overproduction conducted with DHE and DHR123. The effect on mitochondria was determined with complementary criteria: measurement of succinate dehydrogenase activity, evaluation of mitochondrial potential ($\Delta\Psi m$) and mitochondrial superoxide anions ($O_2^{\bullet -}$) production using $DiOC_6(3)$ and MitoSOX, respectively; quantification of mitochondrial mass with Mitotracker Red, and of cardiolipins and organic acids. The effects on mitochondrial and peroxisomal ultrastructure were determined by transmission electron microscopy. Intracellular sterol and fatty acid profiles were determined. Apoptosis and autophagy were characterized by staining with Hoechst 33342, Giemsa and acridine orange, and with antibodies raised against caspase-3 and LC3. DMF and MMF attenuate 7β-OHC-induced cytotoxicity: cell growth inhibition; decreased cell viability; mitochondrial dysfunction (decrease of succinate dehydrogenase activity, loss of $\Delta\Psi m$, increase of mitochondrial $O_2^{\bullet -}$ production, alteration of the tricarboxilic acid (TCA) cycle, and cardiolipin content); oxidative stress induction (ROS overproduction, alteration of GPx, CAT, and SOD activities, increased levels of MDA, CDs, and CPs); changes in fatty acid and cholesterol metabolism; and cell death induction (caspase-3 cleavage, activation of LC3-I in LC3-II). Ultrastructural alterations of mitochondria and peroxisomes were prevented. These results demonstrate that DMF and MMF prevent major dysfunctions associated with neurodegenerative diseases: oxidative stress, mitochondrial dysfunction, apoptosis and autophagy.

Keywords: dimethyl fumarate, monomethyl fumarate, 7β-hydroxycholesterol, 158N cells, oxidative stress, mitochondria, peroxisome, oxiapoptophagy, apoptosis, autophagy, lipid profile.

Introduction

Oxidative stress is characterized by an imbalance between excessive production of reactive oxygen species (ROS) and the capacity of antioxidant defenses to attenuate damage caused by free radicals [1] Oxidative stress is amplified in a variety of neurodegenerative, chronic inflammatory, vascular and neurodegenerative diseases. Thus, several studies have carefully characterized the relationships between oxidative stress and demyelinating and non demyelinating neurodegenerative diseases [2, 3]. Oxidative injury can be involved in brain lesions via the induction of protein and lipid oxidation [4], or mitochondrial dysfunction [5]. In the presence of oxidative stress, the high content of cholesterol in the brain makes it vulnerable to oxidation, which favors the generation of deleterious compounds, named oxysterols (cholesterol oxide products), in the central nerve system (CNS) [6]. Some of these oxysterols (mainly those oxidized on C7, such as 7-ketocholesterol (7KC) and 7β-hydroxycholesterol (7β-OHC), mostly generated by the autoxidation of cholesterol [7]) are known to amplify oxidative stress and mitochondrial damage which contributes to cell death [8]. In humans, 7KC and 7β-OHC levels were increased in the plasma, cerebrospinal fluid (CSF) or postmortem brain tissues of patients with neurodegenerative diseases, including multiple sclerosis (MS) [9], Parkinson's disease [10], Huntington's disease [11] or Alzheimer's disease (AD) [12]. Aβ peptide, a toxic peptide characteristic of AD, was shown to participate in the production of 7β-OHC [13]. It is also known that 7KC can be converted to 7β-OHC [14] by 11β-hydroxyxteroid dehydrogenase type 1 (11β–HSD1) [15]. In humans, the 11β–HSD1 is also able to catalyse the conversion of 7β-OHC into 7KC [14]. As 7β-OHC can be formed from 7KC and vice versa, the deleterious effects of both are closely related. It is therefore important to consider the activities of 7KC and 7β-OHC since these two cytotoxic oxysterols are involved in neurodegeneration [3]. Currently, it has been demonstrated in different cell types from various species [16-19], that 7β-OHC induces a more or less pronounced apoptotic mode of cell death associated with oxidative stress. Later, a complex cell death process defined as oxiapoptophagy ((OXIdative stress, APOPTOsis, autoPHAGY)) was described on microglial cells and oligodendrocytes [8, 20]. This particular type of cell death involving oxidative stress, mitochondrial dysfunction, and induction of apoptosis and autophagy, which are hallmarks of neurodegenerative diseases, was observed in 7β-OHC-treated murine oligodendrocytes 158N [8]. The cellular model used in the present study (murine oligodendrocytes 158N treated with 7β-OHC) is therefore an interesting tool for identifying molecules targeting major cell alterations (oxidative stress and mitochondrial dysfunction leading to cell death) associated with demyelination, since oligodendrocytes are myelin synthesizing cells.

To prevent demyelination, different molecules have been tested for their neuroprotective capacities such as dimethyl fumarate (DMF), the active component of Tecfidera (Biogen) also named BG-12 [21]. DMF is a fumaric acid ester which has immunomodulatory, anti-inflammatory, and antioxidant proprieties [22-24]. This small drug has been approved as an oral therapeutic agent for the treatment of patients with relapsing-remitting MS [25, 26]. Many studies have provided that the pharmacological effect of DMF is due to its bioactive metabolite, monomethyl fumarate (MMF) [21, 27]. This metabolite has beneficial effects on neuroinflammation, neurodegeneration and oxidative stress [23, 28]. It is supposed that DMF and MMF act by the activation of Nrf2 (nuclear factor E2-related factor2) pathway, through the induction of antioxidant protein expression [22]. Under physiological conditions, Nrf2 is sequestered in the cytoplasm through its interaction with the repressor protein 'kelch-like ECH-associated protein 1' (Keap1). Treatment with compounds, like DMF, results in the conformational modifications of cysteine residues on Keap1 [28], which allows activation and nuclear translocation of Nrf2 to promote protective genes such as heme-oxygenase-1 [22] and NADPH-quinone oxidoreductase-1 [28].

In the present study, we evaluated the cytoprotective effects of DMF and MMF on 7β-OHC-treated murine oligodendrocytes 158N. We asked whether DMF and MMF were able to prevent or reduce 7β-OHC-induced cytotoxicity (oxidative stress, mitochondrial dysfunction, modification of lipid profile, apoptosis and autophagy) accompanying demyelination in MS. In addition, as 158N cells express major myelin proteins, proteolipid protein (PLP) and myelin basic protein (MBP) [29], which are major compounds of myelin (a proteolipidic complex which wraps around the axons and is essential for the transmission of nerve impulse) [30], the effects of 7β-OHC in the presence or absence DMF and MMF on PLP and MBP expression were also evaluated.

2. Material and methods

2.1. Cell culture and treatments

Murine oligodendrocyte cells (158N) [29] were cultured in Dulbecco's Modified Eagle Medium (DMEM) (Lonza, Amboise, France) containing 5% (v/v) heat-inactivated fetal bovine serum (FBS) (Dutscher, Brumath, France) and 1% antibiotics (penicillin, streptomycin) (Dutscher). Cells were incubated in a humidified atmosphere (5% CO_2, 95% air) at 37°C and passaged twice a week.

The stock solutions of 7β-hydroxycholesterol (7β-OHC) (Sigma-Aldrich, St Quentin Fallavier, France) was prepared at 800 µg/mL (2 mM) as previously described [19] and stored at 4°C. Dimethyl fumarate (DMF) (ref: 242926, Sigma-Aldrich) and monomethyl fumarate (MMF) (ref: 651419; Sigma-Aldrich) stock solutions, were prepared at 50 mM in DMSO (Sigma-Aldrich). α-Tocopherol (the major

component of Vitamin E; ref: T3251, Sigma-Aldrich) solution was prepared at 80 mM as previously described [19].

In the different experimental conditions, murine oligodendrocytes 158N were seeded either in Petri dishes (30,000 cells/cm^2, 100 mm diameter), or in six-well plates (2.4 x 10^5 cells per well). After 24 h of culture, and for an additional 24 h period of time, DMF (25 µM), MMF (25 µM) or α-tocopherol (400 µM) (used as a positive control for cytoprotection) were introduced in the culture medium 2 h before the addition of 7β-OHC (50 µM). The choice of the concentrations of 7β-OHC (50 µM) as well as of DMF (25 µM) and MMF (25 µM) was based on a study by Ragot et al. [19] and on the dose-effect relationship of 7β-OHC (1, 6.25, 12.5, 25, 50, 100 and 200 µM) (**Supplementary Fig. 1**) and of DMF or MMF in the presence or absence of 7β-OHC (**Supplementary Fig. 2**). With 7β-OHC, the concentration of 50 µM corresponds to the 50 % inhibiting concentration on 158N cells (**Supplementary Fig. 1**). In vitro, it is important to underline that only a part of oxysterols (1-35% depending on the cell type considered) accumulates in the cells [3, 31]., It has been established that the median level of 7β-OHC was 1.11 µg/mL (2.8 µM) and 1.43 µg/mL (3.6 µM) in the cerebrospinal fluid of normal subjects and of patients with multiple sclerosis, respectively [9]. Few data are available on the intracellular level of oxysterols in nerve cells. However, when the oxysterols such as 7β-OHC are used in vitro at µM concentrations (50 µM in the present study), the estimated intracellular levels of this compound are in the range of those found in the frontal and occipital cortex of patients with Alzheimer'disease [12]. Additional experiments were also performed to assess the effect of DMF and MMF in the recovery of 7β-OHC (50 µM)-induced cell death. In these experiments, after 24 h of culture, 158N cells were incubated with 7β-OHC for 6 and 10 h before the addition of DMF or MMF, or α-tocopherol. The cells were further incubated with 7β-OHC in combination with DMF, MMF or α-tocopherol for an additional 14 or 18 h.

2.2. Evaluation of cell morphology by phase contrast microscopy

After treatment of 158N cells with or without 7β-OHC (50 µM) in the presence or absence of DMF (25 µM), MMF (25 µM) or α-tocopherol (400 µM), cell morphology, cell density and cell detachment (loss of cell adhesion) were evaluated by phase contrast microscopy using an inverted-phase contrast microscope (Axiovert 40 CFL, Zeiss, Jena, Germany). Images were obtained with a camera (Axiocam ICm 1, Zeiss).

2.3. Quantification of adherent cells with crystal violet staining

Adherent cells were estimated by staining with crystal violet (Sigma-Aldrich). After treatment of 158N cells, adherent cells were stained with crystal violet for 5 min, rinsed three times with water. Crystal

violet was then dissolved with 0.1 % sodium citrate (Sigma-Aldrich) in 50% ethanol (Carlo-Erba, Val de Reuil, France) and the optical density per well was read at 570 nm with a microplate reader (Tecan Sunrise, Tecan, Lyon, France).

2.4. Evaluation of cell viability with the fluorescein diacetate (FDA) assay

The FDA assay evaluates the ability of living cells to transform the FDA to fluorescein after cleavage by plasma membrane esterases [32]. After 24 h of treatment with or without 7β-OHC (50 µM) in the presence or absence of DMF or MMF (25 µM), 158N cells were incubated for 5 min at 37°C with 50 µM FDA (Sigma-Aldrich), and then lysed with 10 mM of Tris-HCl solution containing 1% sodium dodecyl sulfate (SDS, Sigma-Aldrich). Fluorescence intensity of fluorescein (λ_{Ex} Max: 485 nm, λ_{Em} Max: 528 nm) was measured with a TECAN fluorescence microplate reader (Tecan Infinite M 200 Pro, Lyon, France).

2.5. Cell counting of viable cells with trypan blue

Adherent and non-adherent cells were collected by trypsinization and resuspended in culture medium. The total number of viable cells was determined with a Mallasez counting chamber under a light microscope in the presence of trypan blue (v/v), which stains dead cells in blue.

2.6. Evaluation of plasma membrane permeability and cell death by staining with propidium iodide

Propidium iodide (PI) was used to quantify plasma membrane permeability and cell death [33]. At the end of reatment with or without 7β-OHC (50 µM)) in the presence or absence of DMF (25 µM), MMF (25 µM) or α-tocopherol (400 µM). 158N cells (adherent and non-adherent cells) collected by trypsinization, were stained with 1 µg/mL of PI (5 min at 37°C) and then immediately analyzed with a Galaxy flow cytometer (Partec, Münster, Germany). Fluorescence was collected through a 590/10 bandpass filter on a Galaxy flow cytometer (Partec): 10,000 cells were acquired. Data were analyzed with Flomax (Partec) or FlowJo (Tree Star Inc.) software.

2.7. Mitochondrial analysis

2.7.1. Measurement of mitochondrial succinate dehydrogenase activity with the MTT assay

Mitochondrial activity and/or cell proliferation were evaluated with an MTT based assay. Only metabolically active cells can transform MTT into formazan by mitochondrial succinate dehydrogenase. MTT data was interpreted by comparison with results obtained by cell counting in the

presence of trypan blue. The MTT assay was carried as described previously [34]. The absorbance was read at 570 nm with a microplate reader (TECAN Sunrise, Tecan, Lyon, France).

2.7.2. Measurement of mitochondrial transmembrane potential with $DiOC_6(3)$

The mitochondrial transmembrane potential ($\Delta\Psi_m$) was assessed by flow cytometry with the cationic lipophilic dye 3,3'-dihexyloxacarbocyanine iodide $DiOC_6(3)$ (Thermo Fisher Scientific, Courtaboeuf, France). At the end of treatment, adherent and non-adherent cells were pooled, incubated with $DiOC_6(3)$ (40 nM, 15 min, 37°C) and then analyzed with a Galaxy flow cytometer (Partec) [19, 35]. The loss of transmembrane mitochondrial potential ($\Delta\Psi m$) is indicated by a decreased of the green fluorescence collected through a 520 ± 10 nm band pass filter. For each sample, 10,000 cells were acquired and data were analyzed with Flomax (Partec) or FlowJo (Tree Star Inc.) software.

2.7.3. Measurement of mitochondrial mass with Mitotracker Red

Mitotracker Red (Thermo Fisher Scientific) was used to evaluate mitochondrial mass [36]. Mitotracker Red stock solution was prepared at 1 mM in DMSO. Adherent and non-adherent cells were pooled, washed with DMEM without FBS and then incubated for 30 min at 37°C in a Mitotraker Red solution (100 nM), which was prepared in DMEM without FBS. The fluorescent signals were collected through a 580 ± 20 nm band pass filter on a Galaxy flow cytometer (Partec). Data were analyzed with Flomax software (Partec).

2.7.4. Measurement of mitochondrial reactive oxygen species production with MitoSOX-Red

Mitochondrial production of superoxide anion anion ($O_2^{\bullet-}$) was quantified by flow cytometry after staining with MitoSOX Red (Thermo Fisher Scientific). This positively charged probe accumulates in the mitochondria [36] and exhibits an orange/red fluorescence (λ_{Ex} Max = 510 ; λ_{Em} Max= 580 nm). MitoSOX Red stock solution was prepared at 5 mM in PBS and used at 5 µM in the cells. After cell treatments, adherent and non-adherent cells were pooled by trypsinization and incubated with MitoSOX Red for 15 min at 37°C. The fluorescent signals were collected through a 580 ± 20 nm band pass filter on a Galaxy flow cytometer (Partec). For each sample, 10,000 cells were acquired. Data were analyzed with Flomax software (Partec).

2.7.5. Measurement of mitochondrial cadiolipin levels

The characterisation and quantification of cardiolipins was conducted by liquid chromatography tandem-mass spectrometry (LC-MS/MS) on an Agilent 6460 QqQ (Agilent Technologies, Santa Clara, CA, USA). Total lipid was extracted from cell pellet as described previously by Folch et al. [37], then

dissolved in 100 µL of chloroform/methanol/water mixture. About 1 to 8 µL of extacted lipid were used for lipidomic analysis. Lipid standards and chemicals of the highest grade available were from Avanti Polar Lipids (Coger SAS, Paris, France) and Sigma-Aldrich, respectively. LC-MS/MS quality grade solvents were from Thermo Fischer Scientific. Extracted lipids for cardiolipin analysis were determined as described previously by Vial et al. [38].

2.8. Mass spectrometry analysis of sterols, fatty acids phospholipids and organic acids

Total lipid was extracted by the Folch's method [37], and fatty acids, sterols and organic acids were quantified as described previously [31, 39, 40]. Gas chromatography-mass spectrometry (GC-MS) analysis was performed on a Clarus 600D (Perkin Elmer, USA). The GC was equipped with an Elite column (30 m x 0.32 mm id x 0.25 mm film; Perkin Elmer) and injection was performed in splitless mode using helium (1 mL/min) as carrier gas. The temperature program was as follows: initial temperature of 80°C was held for 1 min, followed by a linear ramp of 10°C/min to 220°C, 20°C/min to of 280°C and 5°C/min up to 290°C, which was held for 10 min. The mass spectrometer operates in full mass scan or selected ion-monitoring mode. Peak integration was performed manually, and metabolites were quantified from selected-ion monitoring analyses against internal standards using standard curves for all the compounds [39, 40]. For phospholipid analysis, total lipid was also extracted by the Folch's method [37]; phosphatidylcholine and sphingomyelin were quantified as described previously [19].

2.9. Evaluation of oxidative stress

2.9.1. Analysis of antioxidant enzymes activities: catalase, glutathione peroxidase (GPx) and superoxide dismutase (SOD)

Catalase (CAT) activity was determined by photometric measurement of H_2O_2 consumption at 240 nm. 158N cells were trypsinized, washed with PBS, and lysed in RIPA buffer (10 mM Tris-HCl, pH 7.2, 150 mM NaCl, 0.5% Nonidet NP40, 0.5% Na deoxycholate, 0.1% SDS, 2 mM EDTA and 50 mM NaF) in the presence of 1/25 complete protease inhibitor cocktail tablets (Roche Diagnostics, Indianapolis, IN, USA) for 30 min on ice. Cell lysates were collected after centrifugation at 12,000 g for 20 min at 4°C. The reaction was initiated by the addition of Tris-HCL (1 M, pH 7.4), and H_2O_2 (400 mM), andthe amount of H_2O_2 remaining after 2 min was measured spectrophotometrically (240 nm), using a microplate reader (Tecan Infinite M 200 Pro).

Glutathione peroxydase (GPx) activity was quantified as previously described [41]. 158N cells were lysed by sonication and centrifuged at 20,000 g for 30 min at 4°C. Cell lysates were incubated for 5 min at 25°C with 0.1 mM reduced glutathione (GSH) and phosphate buffer saline (50 mM, pH 7.8).

The reaction mixture was initiated by addition of H_2O_2 and stopped by the incubation with 1% trichlorric acid, for 30 min at 4°C, and then centrifuged at 1,000g for 10 min. The absorbance was measured at 412 nm (Lambda 25 Spectrophotometer, Perkin Elmer, Villebon sur Yvette, France).

Superoxide dismutase (SOD) activity was quantified using the method of Misra and Fridovich [42]. This colorimetric assay, evaluates the ability of SOD to inhibit the Cytochrome c-reduction, induced by superoxide anions produced by xanthine oxidase enzyme [34]. To this end, cell lysates were added to potassium phosphate buffer (0.05 M, pH 7), and 50 µM xanthine (ref 69-89-6, Sigma-Aldrich). Then 0.01U of xanthine oxidase (ref 9002-17-9, Sigma–Aldrich) and 5 µM of cytochrome c were added. Absorbance was measured at 550 nm at 20 min intervals for at least five reading. Antioxidant enzyme activities were expressed relative to the protein content determined with the Bradford method.

2.9.2. Measurement of thiol (SH group) levels

Measurement of thiols (SH group) was conducted according to the method of Flaure & Lafon [43]. Cellular lysates were mixed with 5-5'DiThiobs-(2-NitroBenzoic acid) (DTNB), and incubated in dark for 15 min. The absorbance was measured at 415 nm on a Lambda 25 Spectrophotometer (Perkin Elmer).

2.9.3. Measurement of reactive oxygen species (ROS) overproduction with dihydroethidium and dihydrorhodamine 123

ROS overproduction, including superoxide anion ($O_2^{\bullet -}$), was quantified by flow cytometry after staining with dihydroethidium (DHE; Thermo Fisher Scientific) used at 2 µM. Once in the cell, DHE is rapidly oxidized and exhibits an orange fluorescence (λ_{Ex} Max= 488 nm; λ_{Em} Max= 575 nm) [44]. ROS overproduction, including hydrogen peroxide (H_2O_2), was also detected with dihydrorhodamine 123 (DHR 123, Cliniscience, Nanterre, France) used at 6 µM, which is oxidized to Rhodamine 123 (RH123) (λ_{Ex} Max = 505 nm; λ_{Em} Max = 529 nm) [45]. After 24 h of treatment, adherent and non-adherent cells were stained with DHE or DHR123 and incubated at 37°C for 15 min. Fluorescent signals were collected with 590 ± 20 nm (DHE) and 520 ± 20 nm (DHR 123) band pass filters, respectively. Ten thousand cells were acquired from each sample. Data were analyzed with Flomax (Partec) or FlowJo (Tree Star Inc.) software.

2.9.4. Measurement of lipid peroxidation products: conjugated dienes (CDs) and malondialdehyde (MDA)

Conjugated dienes (CDs) are the products of polyunsaturated fatty acid peroxidation. The level of CDs was determined with the method of Esterbauer et al. [46]. Malondialdehyde (MDA) is a lipid peroxidation product. It is an alkylating agent capable of reacting with biologic macromolecules. The

level of MDA was evaluated as previously described [47]. The experimental procedures on 158N cells were performed as described previously [31].

2.9.5. Measurement of carbonylated proteins (CPs) level

Similarly than lipids, proteins can also be oxidized. The measurement of carbonylated proteins (CPs) level was conducted as described by Oliver et al. [48]. This method, which is based on the reaction of 2, 4-dinitrophenylhydrazine (DNPH) with CP groups to form protein hydrazones, was realized as previously described [31].

2.10. Cell death characterization

2.10.1. Evaluation of cell death by the measurement of lactate dehydrogenase activity

The culture medium of 158N cells treated with or without 7β-OHC (50 µM) in combination with with DMF (25 µM), MMF (25 µM) or α-tocopherol (400 µM) were collected, and centrifuged to eliminate non adherent cells. Lactate dehydrogenase (LDH) activity was quantified using a commercial kit (#ab102526, Abcam, Paris, France). A microplate reader (TECAN Infinite M 200 Pro) was used to measure LDH activity at a wavelength of 450 nm in a kinetic mode at 25°C for 30-60 min.

2.10.2 Characterization of cell death by the evaluation of nuclear morphology after staining with Giemsa or Hœchst 33342

Normal and apoptotic versus necrotic cells can be identified by nuclear morphology evaluated after staining with Giemsa and/or Hœchst 33342 as described previously [33]. Apoptotic cells were characterized by condensed and/or fragmented nuclei whereas normal cells have regular and round nuclei. A total of 300 cells per sample were counted to determine the percentage of apoptotic cells.

2.10.3. Measurement of lysosomal destabilization with Acridine Orange

Acridine orange (AO) was used to evaluate lysosomal integrity [49] and or to quantify autophagic vesicular (acidic vesicular) formation [50-52]. AO stock solution was prepared at 1 mg/mL in DMSO and used at 1 µg/mL. After 15 min of incubation at 37°C, cells were washed, and resuspended in PBS for flow cytometry analysis. The fluorescence of AO was collected using a 630 nm longpass filter and measured on a logarithmic scale. Ten thousand cells were acquired on a Galaxy flow cytometer (Partec). Data were analyzed with Flomax (Partec) or FlowJo (Tree Star Inc.) software.

2.10.4. Polyacrylamide gel electrophoresis and Western blotting

Adherent and floating cells were harvested and lysed for 30 min on ice in a RIPA buffer (10 mM Tris-HCl, pH 7.2, 150 mM NaCl, 0.5% Nonidet NP40, 0.5% Na deoxycholate, 0.1% SDS, 2 mM EDTA and 50 mM NaF) containing a complete protease inhibitor cocktail (Roche Diagnostics, Indianapolis, IN, USA). The cell debris were eliminated by centrifugation (20 min, 10,000 g), and the supernatant was collected. The protein concentrations were measured using bicinchoninic acid reagent (Sigma Aldrich). Seventy micrograms of protein were diluted in a loading buffer (125 mM Tris-HCl, pH 6.8, 10% β-mercaptoethanol, 4.6% SDS, 20% glycerol, and 0.003% bromophenol blue), separated on a SDS-PAGE gel, and transferred onto a nitrocellulose membrane (Thermo Fischer Scientific). Nonspecific binding sites were blocked by incubation with 5% milk powder in PBST (PBS, 0.1% Tween 20, pH 7.2) and the membranes were incubated overnight at 4°C with the primary antibody diluted in 5% milk in PBST. For apoptosis and autophagy analysis, the antibodies used were directed against caspase-3 (Ozyme / Cell Signaling (# 9662) (for detection of the endogenous level of full length caspase-3 (35 kDa) and its large cleavage product (17 kDa)), and LC3-I/II (#L8918, Sigma Aldrich) (detecting LC3-I (18 kDa) and LC3-II (16 kDa)), respectively; all antibodies were rabbit polyclonal antibodies; they were used at a final dilution of 1/1000. For myelin protein analysis (proteolipid protein (PLP); myelin basic potein (MBP)), PLP expression was determined with a rabbit polyclonal antibody (PLP; Novus, NB10074503) and MBP expression with a mouse monoclonal antibody (MBP; Millipore, MAB381). An antibody directed against β-actin (mouse monoclonal antibody (#A2228, Sigma Aldrich)) was used at a final concentration of 1/10,000. Membranes were washed three times for 5 min, with PBST and incubated for 1 h at room temperature with horseradish peroxidase-conjugated goat anti-rabbit (for caspase-3, LC3-I/-II, and PLP) diluted at 1/5,000 in 1% milk powder in PBST or anti-mouse antibody against MBP or β-actin, diluted at 1/5,000 in 1% milk powder in PBST. The membranes were then washed and antibody binding revealed using an enhanced chemiluminescence detection kit (Supersignal West Femto Maximum Sensitivity Substrate, Thermo Fisher Scientific) and Chemidoc XRS+ (Bio-Rad, Marnes la Coquette, France). Band intensity was determined with Image Lab software (Bio-Rad). The expression of caspase-3 (uncleaved and cleaved) and the ratio LC3-II / LC3-I were calculated with Image Lab software (Bio-Rad). The expression of caspase-3 and the level of cleaved caspase-3 were normalized versus β-actin, and expressed as normalized expression versus control (untreated cells). The ratio LC3-II / LC3-I was calculated for each assay.

2.10.5. Evaluation of the activation of PKA, PKC and MEK / ERK signalling pathways in 7β-hydroxycholesterol-treated 158N cells

To evaluate the signalling pathways activated during 7β-OHC-induced cell death, different inhibitors were used. To this end, 158N cells were seeded in 24 wells at 60,000 cells / well. After 24 h of culture, 158N cells were cultured in the presence or absence of 7β-OHC (50 µM) with or without different inhibitors such as H89 (20 µM, Sigma-Aldrich), U73122 (1 µM, Sigma-Aldrich), chelerythrine (1 µM, Sigma-Aldrich), and U0126 (20 µM, Calbiochem, San Diego, CA, USA), which inhibit protein kinase A (PKA), phospholipase C (PLC), protein kinase C (PKC) and MEK, respectively. These inhibitors were choosen for the following reasons: cAMP level leading to PKA activation is increased during during 7β-OHC-induced cell death; a cytosoloic Ca^{2+} increase contributing to PLC activation is observed during 7β-OHC-induced cell death; and 7β-OHC-induced cell death is associated with inflammatory cytokines overproduction as well as enhanced expression of integrins via the activation of the nuclear factor κB (NF- κB) involving PKC and MEK-ERK signalling pathways [16, 18]. These compounds were introduced in culture medium 30 min before the 7β-OHC. Stock solutions of these inhibitors were prepared as follow: the H89 stock solution was prepared in distilled water at 1 mM, while U0126 (0.1 mM), U73122 (0.1 mM) and chelerythrine (1 mM) stock solutions were prepared in DMSO. At the end of the treatments, an FDA assay was carried out as described previously.

2.11. Quantification of 11β-hydroxyxteroid dehydrogenase type 1 (11β–HSD1) and 11β-hydroxyxteroid dehydrogenase type 2 (11β–HSD2) by RT-qPCR

11β-HSD1 is an intracellular enzyme that catalyzes interconversion of cortisone in cortisol [53]. 11β–HSD1 also catalyses the conversion of 7KC to 7β-OHC and reciprocally [54, 55]. However, the conversion of 7β-OHC to 7KC can also be catalyzed by 11β–HSD2 [56]. Total mRNA from 158N cells (and microglial BV-2 cells used as positive control [20]) were extracted and purified using the RNeasy Mini Kit (Qiagen, Courtaboeuf, France). Total mRNA concentration was measured with TrayCell (Hellma, Paris, France). The purity of nucleic acids was controlled by the ratio of absorbance at 260 nm and 280 nm (ratios of 1.8 - 2.2 were considered satisfactory). One microgram of total mRNA was used for reverse transcription with the iScript cDNA Synthesis Kit (Bio-Rad) according to the following protocol: 5 min at 25°C, 20 min at 46°C, 5 min at 95°C. cDNA was amplified using the FG Power SYBR Green (Thermo Fischer Scientific). All PCR reactions were performed on an Applied Biosystem Step One plus QPCR machine (Life Science Technologies). The primer sequence of *11β–HSD1* was:

- *11β–HSD1: forward 5'-actcagacctcgctgtctct-3' and reverse 5'-gcttgcagagtagggagcaa-3'*
- *11β–HSD2: forward 5'*-ggttgtgacactggttttggc-*3' and reverse 5'*-agaacacggctgatgtcctct-*3'*

Thermal cycling conditions were as follows: activation of DNA polymerase at 95°C for 10 min, followed by 40 cycles of amplification at 95°C for 15 s, 60°C for 30 s, and 72°C for 30 s, followed by

a melting curve analysis to test for the absence of non-specific products. Gene expression was quantified using cycle to threshold (Ct) values and normalized by the *36B4* reference gene (*forward 5'-gcgacctggaagtccaacta-3' and reverse 5'-atctgcttggagcccacat-3'*). The quantitative expressions of *11β–HSD1 and 11β–HSD2* were determined as fold induction above the control.

2.12. Statistical analysis

Statistical analyses were performed using the Statview Software (SAS Institut Inc, NC, USA) using a one way or a two way analysis of variance (ANOVA) followed by Student's t-test. Data shown are the mean ± standard deviation (SD) of two or three independent experiments, usually conducted in triplicate. Data were considered statistically significant at a P-value of 0.05 or less.

3. Results

3.1. Effects of dimethyl fumarate and monomethyl fumarate on the adhesion and morphology of 158N cells

158N cells treated with 7β-OHC are a relevant model to evaluate the relationship between oxidative stress, apoptosis and autophagy (oxiapoptophagy); to specify the role played by mitochondria, in this process; and to identify natural or synthetic molecules capable of preventing the toxic effects of 7β-OHC associated with major age-related and neurodegenerative diseases. To evaluate the cytoprotective activity of DMF and MMF on 7β-OHC-treated 158N cells, these cells were cultured for 24 h with or without 7β-OHC (50 µM, 24 h) in the presence or absence of DMF and MMF, used at 25 µM. α-tocopherol (400 µM) was choosen as positive cytoprotective control. The effects of DMF and MMF were evaluated compared to untreated cells (control) and vehicle-treated cells (ethanol 0.6% or DMSO 0.05%).

Based on the observations performed by phase contrast microscopy, morphological changes were identified under treatment with 7β-OHC: a pronounced increase of the number of round and floating cells, indicating of loss of cell adhesion and an induction of cell death, was observed; whereas only few non adherent cells were present in control and vehicle-treated cells **(Fig 1A)**.Of note, when 7β-OHC was associated with DMF, MMF or α-tocopherol, the loss of cell adhesion was prevented and an important decreases of the number of non adherent cells was observed. (**Fig 1A**).

The impact of DMF and MMF on cell adhesion was confirmed by the crystal violet assay. Under treatment with 7β-OHC and compared to control and vehicle-treated cells, a significant decrease of adherent cells was revealed **(Fig. 1B)**. When 7β-OHC was associated with DMF and MMF the percentage of adherent cells was significantly increased: DMF and MMF increased by 30-32% the

428 percentage of adherent cells, respectively. This effect is comparable to those observed with α-
429 tocopherol **(Fig. 1B)**.
430
431 **3.2. Effects of dimethyl fumarate and monomethyl fumarate on plasma membrane integrity and**
432 **cell viability**
433 The impact of DMF and MMF on 7β-OHC-induced loss of plasma membrane integrity and on cell
434 death induction was determined on 158N cells. To this end, 158N cells were stained either with
435 fluoresceine diacetate (FDA), propidium iodide (PI) or trypan blue, and in addition LDH was
436 measured in the culture medium.
437 After staining with FDA, a significant decrease of FDA positive cells (FDA+ cells) was observed in
438 7β-OHC-treated cells compared to the corresponding vehicle and to the control (**Fig. 2A**). With the
439 trypan blue assay, a significant decrease of the total number of living cells was simultaneously
440 observed with 7β-OHC. Compared to 7β-OHC, co-treatment with DMF or MMF induced a significant
441 increase of almost 40% of (FDA+ cells) as well as an increase of the total number of living cells
442 evaluated after staining with trypan blue. More pronounced cytoprotective effects were seen with α-
443 tocopherol **(Fig. 2A-B)**.
444 After staining with PI, in the presence of 7β-OHC, more than 70% of propidium iodide positive cells
445 (PI +) were observed, indicating an increased permeability of the plasma membrane to PI which stains
446 cells with damaged plasma membranes, often corresponding to dead cells (**Fig. 2C**). The increase of
447 permeability to PI was strongly attenuated by DMF and MMF (**Fig. 2C**).
448 In addition, the quantification of LDH acitivity in the culture medium, which is a criteria of cell death,
449 showed an increased LDH activity in 7β-OHC-treated cells (**Fig. 2D**). This increase was strongly
450 attenuated by DMF and MMF; in the culture medium of (7β-OHC + DMF) or (7β-OHC + MMF), the
451 LDH activity was only slightly higher than in control and vehicle-treated cells (**Fig. 2D**).
452 Of note, the ability of DMF and MMF to prevent the decrease of FDA+ cells and of living cells, as
453 well as the increase of PI+ cells was similar to that observed with α-tocopherol **(Fig. 2)**.
454
455 **3.3. Effects of dimethyl fumarate and monomethyl fumarate on 7β-hydroxycholesterol-induced**
456 **oxidative stress**
457 To determine the ability of DMF and MMF to prevent 7β-OHC-induced oxidative stress, we studied
458 the impact of these fumarate esters on the production of reactive oxygen species (ROS: $O_2^{\bullet -}$, H_2O_2),
459 antioxidant enzyme (SOD, CAT, GPx) activities, and macromolecule oxidation products (MDA,
460 carbonylated proteins) as well as on the level of SH-groups and conjugated dienes (CDs).

The measurement of ROS production was evaluated by flow cytometry after staining with DHE and DHR123. The highest percentage of DHE and DHR123 positive cells was observed when 158N cells were exposed to 7β-OHC compared to control and vehicle-treated cells. This increase was significantly inhibited when 7β-OHC was associated with DMF and MMF **(Fig. 3).** The most important attenuation of 7β-OHC-induced ROS overproduction was observed with α-tocopherol used as positive control anti-oxidant molecule (**Fig. 3**).

Under treatment with 7β-OHC, a significant increase of GPx, SOD, and CAT activities was observed compared to control and vehicle-treated cells **(Fig. 4A-C).** Compared to 7β-OHC-treated cells, GPx, SOD and CAT activities were significantly increased when 7β-OHC was associated with DMF or MMF, and the most important increase was observed with DMF (**Fig. 4A-C**). In the presence of α-tocopherol, the effects were similar to those of DMF and MMF. On the otherhand, a significant decrease in the level of SH-groups was observed in 7β-OHC-treatd cells compared to control and vehicle-treated cells (**Fig. 4D**).Of note, the level of SH-groups was almost normalized, and in the range of that measured in control and vehicle-treated cells, when 7β-OHC was associated with DMF, MMF and α-tocopherol **(Fig. 4D)**. With biochemical colorimetric methods of analysis, allowing evaluation of lipid and protein oxidation products, a significant increase of CDs, MDA, and carbonylated proteins levels (CPs) which are biomarkers of lipid and protein oxidation, was observed when 158N cells were exposed to 7β-OHC compared to control and vehicle-treated cells **(Fig. 5A-C)**. Interestingly, this increase was significantly attenuated when 7β-OHC was associated with DMF and MMF **(Fig. 5A-C)**. Similar effects than DMF and MMF were found in the presence of α-tocopherol (**Fig. 5**).

3.4. Effects of dimethyl fumarate and monomethyl fumarate on 7β-hydroxycholesterol-induced mitochondrial damage and peroxisomal changes

As mitochondrial damage is induced by 7β-OHC in 158N cells, the impact of DMF and MMF at the mitochondrial level was studied. To this end, succinate dehydrogenase activity, transmembrane mitochondrial potential (ΔΨm), mitochondrial mass, superoxide anions ($O_2^{\bullet -}$) production, and cardiolipin levels were evaluated.

The MTT assay, used to measure succinate dehydrogenase activity, showed that the ratio [(% MTT positive cells in the assay) / (% MTT positive cells in the control)] was significantly reduced with 7β-OHC compared to control and ethanol-treated cells **(Fig. 6A)**. When 7β-OHC was associated with DMF and MMF this ratio was significantly increased. A similar effect was observed with α-tocopherol. These data showed that DMF and its main metabolite MMF prevent the decrease of succinate dehydrogenase activity which participates in both the TCA cycle and the electron transport chain at the mitochondrial level. These data lead us to examine the effect of DMF and MMF on 7β-

OHC-induced loss of transmembrane mitochondrial potential (ΔΨm) on 158N cells by staining with $DiOC_6(3)$. A high value (33%) of $DiOC_6(3)$ negative cells, indicating a decrease in ΔΨm (cells with depolarized mitochondria) was detected under treatment with 7β-OHC **(Fig. 6B)**. The percentage of $DiOC_6(3)$ negative cells was strongly reduced when 158N cells were co-treated with DMF, MMF or α-tocopherol (**Fig. 6B**). Another fluorochrome (MitoTracker Red) was used to evaluate the mitochondrial mass. Upon staining with Mitotracker Red, an increase in the mean fluorescence intensity (MFI) of this dye was observed when the cells were treated with 7β-OHC compared to control and vehicle-treated cells (**Fig. 6C**). This increase was significantly inhibited by DMF and MMF, as well as by α-tocopherol **(Fig 6C**).

Due to the important role played by cardiolipins, which are essential mitochondrial phospholipids for electron transport, oxidative phosphorylation and energy production [57, 58], it was important to determine the effect of 7β-OHC on the cardiolipin content. No difference in cadiolipin content was observed between untreated cells (control) and vehicle-treated cells (**Fig. 6D**). The highest levels of cardiolipins was found with DMF and MMF (**Fig. 6D**). Total cardiolipin content was significantly decreased in 7β-OHC-treated cells compared to control and vehicles-treated cells (**Fig. 6D**), When 7β-OHC was associated with DMF and MMF, this decrease was counteracted and the cardiolipin values observed were in the range of that observed in control and vehicle-treated cells (**Fig. 6D**). The same observation was made with α-tocopherol **(Fig. 6D**).

In addition, flow cytometric analyses were performed with MitoSOX allowing the measurement of $O_2^{\bullet -}$ production at the mitochondrial level (MitoSOX positive cells). In cells incubated with 7β-OHC compared control and to vehicle-treated cells an overproduction of $O_2^{\bullet -}$ was observed. This overproduction of $O_2^{\bullet -}$ was counteracted by DMF, MMF and α-tocopherol **(Fig. 6E**).

As mitochondria and peroxisome are tightly connected organelles [59], the effects of 7β-OHC on the peroxisome was evaluated by transmission electron microscopy (**Fig. 7**). Whereas round peroxisomes were mainly observed in control cells, several peroxisomes with irregular shapes, which were often larger or smaller than in the control, were detected in 7β-OHC-treated cells **(Fig. 7)**. Several mitochondria, which were smaller than in control cells, were also frequently observed in 7β-OHC-treated cells **(Fig. 7).** Of note, these modifications of the peroxisomal and mitochondrial morphologies were prevented when 7β-OHC was associated with DMF **(Fig. 7)**.

Altogether, our data demonstrate that 7β-OHC induced several types of mitochondrial damage, and that DMF and MMF have strong cytoprotective effects at the mitochondrial level.

3.5. Impact of 7β-hydroxycholesterol, dimethyl fumarate, and monomethyl fumarate on cell metabolism

3.5.1. Effects of 7β-hydroxycholesterol, dimethyl fumarate, and monomethyl fumarate on glycolysis and TCA cycle

TCA cycle, also known as Krebs cycle, is the metabolic pathway used to release stored energy through the oxidation of acetyl-CoA, to provide the reducing agent NADH and precursors of certain amino acids. Thic cycle takes place in the matrix of the mitochondria. Thus, we considered pertinent to understand the impact of 7β-OHC, DMF, MMF and 7β-OHC associated with DMF or MMF on the TCA cycle. Lactate dehydrogenase (LDH) converts two pyruvates into 2 lactate molecules, using NADH as a coenzyme so that the cell can continue to perform glycolysis by regenerating NAD^+. The effect of 7β-OHC, DMF, MMF and 7β-OHC associated with DMF or MMF on these metabolic pathways was also evaluated. When exposed to 7β-OHC, a significant increase in lactic acid (lactate) levels was observed (220.59 ± 2.50 ng/million cells) compared to vehicle - treated cells (EtOH 0.6%: 122.64 ± 3.53 ng/million cells); this increase in lactic acid was significantly reduced, under treatment with DMF and MMF in the presence of 7β-OHC (**Table 1**). However, a marked and significant decreases in pyruvic acid (pyruvate), succinic acid (succinate), fumaric acid (fumarate), malic acid (malate) and citric acid (citrate) levels were observed in 7β-OHC-treated 158N cells compared to vehicle; this decrease was attenuated when the cells were simultaneously treated with 7β-OHC and DMF or MMF (**Table 1**).

3.5.2. Effects of 7β-hydroxycholesterol, dimethyl fumarate, and monomethyl fumarate on cholesterol metabolism

In the presence of 7β-OHC, the cholesterol level was significantly decreased compared to vehicle-treated cells (**Table 2**). This reduction of the cholesterol level was still observed when the cells were simultaneously treated with 7β-OHC and MMF (**Table 2**). Compared to 7β-OHC-treated cells, the cholesterol level was significantly increased, when the cells were co-treated with 7β-OHC and DMF (**Table 2**). When cholesterol precursors were measured after treatment with 7β-OHC**,** significant reduced levels of lathosterol, desmosterol, and lanosterol were observed compared to control and vehicle (EtOH 0.6%)-treated cells (**Table 2**). While lanosterol level was normalized with DMF and MMF, a most important decrease of other cholesterol precursors levels was detected (**Table 2**). In addition, cholesterol auto-oxidation products (triol, ketocholesterol (7KC) and 7β-hydroxycholesterol (7β-OHC)) were measured in the same conditions. In 158N cells treated with 7β-OHC, important levels of this oxysterol were found supporting an accumulation and/or an interaction of this compounds with the cells (**Table 2**). After 24 h of incubation with 7β-OHC, the levels of this oxysterol present in the cells (when 158N cells were only cultured in the presence of 7β-OHC) represents 1% of the quantity of 7β-OHC introduced in the culture medium (**Table 2**). This accumulation is lower than

563 those reported with 7KC and 27-hydroxycholesterol which represents 10-20% of the quantity of
564 oxysterols initially introduced in the culture medium [3]. It is noteworthy that in the plasma of X-ALD
565 patients, the concentration of 7β-OHC can reach 2.5 µM [20]. In the presence of 7β-OHC, in
566 agreement with the ability of 7β-OHC to stimulate the oxidative stress, higher levels of triol and 7KC
567 were also observed compared to control cells and vehicle-treated cells; this increase was significantly
568 reduced when 7β-OHC was associated with DMF or MMF (**Table 2**). Despite the levels of triol and
569 7KC being significantly reduced, when 7β-OHC was cultured in the presence of DMF or MMF, the
570 levels of 7β-OHC remained increased, and were even higher than in cells only treated with 7β-OHC
571 (**Table 2**). Therefore, DMF and MMF inhibit the signaling pathways leading to 7β-OHC-induced
572 cytotoxicity without preventing the cellular accumulation of this oxysterol. In 158N cells, the Ct value
573 of the gene HSD11B1 encoding for the enzyme 11β-HSD1 ($Ct_{(HSD11B1)}$ = 36.5 ± 1.0) was high
574 whereas the Ct value of the reference gene 36B4 was low ($Ct_{(36B4)}$ = 18.4 ± 0.1) supporting a good
575 expression of 36B4 in 158N cells (**Supplementary Fig. 3**). In 158N cells, the gene HSD11B1
576 encoding for the enzyme 11β-HSD1 can be considered as non expressed since multiple peaks were
577 observed on the melt curve demonstrating a non specific amplification (**Supplementary Fig. 3**).
578 However, on microglial BV-2 cells, used as positive control, the Ct value of the gene HSD11B1
579 encoding for 11β-HSD1 was higher ($Ct_{(HSD11B1)}$ = 30.2 ± 0.6) than in 158N cells ($Ct_{(HSD11B1)}$ = 36.5 ±
580 1.0); as a melt curve with homogeneous peaks was observed, this supports that BV-2 express the gene
581 of 11β-HSD1 and that the primer sequences used are appropriated (**Supplementary Fig. 3**). According
582 to these data, our results do not support a conversion of 7KC in 7β-OHC, and reciprocally via 11β-
583 HSD1, in 158N cells. Since 7β-OHC can be converted to 7KC by the enzyme 11β-HSD2, the
584 expression of the HSD11B2 gene encoding this enzyme was quantified on both 158N (Ct=26.0 ± 0.6)
585 and BV-2 (Ct=29.3 ± 0.3) (**Supplementary Fig. 4**). The Ct values and the appearance of the melt
586 curves are in favor of an expression of the HSD11B2 gene in these cells. This suggests that in 158N
587 cells, 7β-OHC could be converted to 7KC, especially when the cells are co-treated with 7β-OHC
588 associated with DMF or MMF. The expression of the HSD11B2 gene, which is decreased in the
589 presence of 7β-OHC, evokes that of the control when the cells are cultured in the presence of 7β-OHC
590 associated with DMF or MMF (**Supplementary Fig. 4**).
591
592 **3.5.3. Effects of 7β-hydroxycholesterol, dimethyl fumarate and monomethyl fumarate on the**
593 **cellular fatty acid profile**
594 In order to identify the effects of 7β-OHC, DMF, MMF, and 7β-OHC with or without DMF and MMF
595 on fatty acid metabolism, fatty acid profiles were determined.

As shown in **Table 3**, 7β-OHC induced a significant decrease inthe total long chain saturated fatty acids (∑SFA (C<22)) compared to vehicle-treated cells. A significant decrease in myristic acid (C14:0), palmitic acid (C16:0), stearic acid (C18:0), and arachidic acid (C20:0) levels was observed in 7β-OHC-treated 158N cells compared to the vehicle-treated cells. However, under treatment with 7β-OHC, the total very long chain saturated fatty acid ((∑VLCSFA C≥22) level was 3 times higher than in the vehicle treated cells. Thus, behenic acid (C22:0), tetracosanoic acid (C24:0), and cerotic acid (C26:0) levels were significantly enhanced in 7β-OHC-treated cells compared to vehicle. When 158N cells were co-tretaed with MMF and 7β-OHC, all SFA levels were in the range of untreated and vehicle-treated cells (**Table 3**). However, when 158N cells were co-treated with DMF and 7β-OHC, only C18:0, C22:0 and C26:0 levels were normalized (**Table 3**).

As shown in **Table 4**, 7β-OHC also induced a significant decrease in the total mono-unsaturated fatty acid (∑MUFA) compared to vehicle-treated cells. Thus, myristoleic acid (C14:1 n-5), sapienic acid (C16:1 n-10), palmitoleic acid (C16:1 n-7), eicinoneic acid (C20:1 n-9), and eicisenoic acid (C20:1 n-7) levels were significantly decreased in 158N treated with 7β-OHC compared to vehicle-treated cells; however, under the same conditions, very long chain monounsaturated fatty acids such as nervonic acid (C24:1 n-9) and hexacosaenoic acid (C26:1 n-9) levels were enhanced (**Table 4**). MMF and DMF had almost similar effects on the MUFA profile when used 2 h prior the incubation with 7β-OHC. In fact, all the MUFA levels came closer to those of the untreated cells or vehicle treated cells, with the exception of C16:1 n-10 or n-9 and C16:1 n-7, of which levels were higher even than control and vehicle treated cells. Interestingly when added alone, these molecules (DMF and MMF) and in particular MMF were able to significantly enhance levels of several MUFA compared to the corresponding vehicle.

As shown in **Table 5**, 7β-OHC induced a significant decrease of all polyunsaturated fatty acid (PUFA) levels compared to vehicle-treated cells; thus, total PUFA content was reduced by about half in the cells. When DMF and MMF were used alone on 158N cells, linoleic acid (C18:2 n-6), arachidonic acid (AA; C20:4 n-6), and docosahexaenoic acid (DHA; C22:6 n-3) were enhanced, compared to corresponding to the vehicle. Co-treatment of 7β-OHC with DMF and MMFinduced a correction of all PUFA levels which are in the range of vehicle treated cells (**Table 5**), with the expection of (C20:4 n-6) and eicosapentaenoic acid (EPA; C20:5 n-3), which remained lower than in vehicle- and 7β-OHC-treated cells.

Furthermore, Δ4-desaturase (C22:6 n-3/C22:5 n-3), Δ8-desaturase (C20:3 n-6 /C20:2 n-6), Δ9-desaturase (C18:1 n-9/ C18:0), andelongase activity index (C22:5 n-3 /C20:5 n-3) activity index were significantly increased in 7β-OHC-treated cells (**Table 5**). Compared to 7β-OHC, these indices were significantly reduced when the cells were co-treated with 7β-OHC associated with DMF and MMF.

The elongase (C18:0/C16:0) activity index was higher in 7β-OHC cells comparatively to (7β-OHC + DMF); however, it was reduced in (7β-OHC + MMF) compared to 7β-OHC (**Table 5**).

Our results demonstrated the impact of 7β-OHC on fatty acid metabolism, which could be at least in part, due to mitochondrial damage, since this organelle plays important roles in fatty acid anabolism and catabolism. Our data also demonstrate that DMF and MMF prevent fatty acidsmetabolic disorders in 7β-OHC-treated cells.

3.5.4. Effects of 7β-hydroxycholesterol, dimethyl fumarate and monomethyl fumarate on sphingomyelin and phosphatidylcholine content

The effects of 7β-OHC, DMF, MMF, and 7β-OHC with or without DMF orMMF on the cell content in sphingomyelin (SM) and phosphatidylcholine (PC) were determined by GC/MS. In the presence of 7β-OHC, significant decreases in SM and PC were observed comparatively to control (untreated cells), vehicle-treated cells (EtOH 0.6% or DMSO 0.05%), α-tocopherol, DMF and MMF (**Fig. 8**). Whereas α-tocopherol either failed to, or had a minor effect in preventing the 7β-OHC-induced decreased of SM and PC, respectively, DMF was more efficient than MMF at attenuating the decrease of SM and PC under treatment with 7β-OHC (**Fig. 8**).

3.6. Effects of 7β-hydroxycholesterol with or without dimethyl fumarate and monomethyl fumarate on apoptosis and autophagy

The oxidative stress induced by 7β-OHC in 158N cells was associated with characteristic features of apoptotosis and autophagy, in agreement with previous studies showing that 7β-OHC triggers an oxiapoptophagic mode of cell death on 158N cells [8] (**Fig. 9**). Apoptosis is morphologically characterized by the presence of cells with condensed and/or fragmented nuclei (**Fig. 9A**) and by an induction of cleaved caspase-3 (**Fig. 10**). The occurrence of autophagy is supported by an enhancement of the percentage of acridine orange (AO)-positive cells (**Fig. 9B**), which could correspond to the presence of cells with large and/or numerous autophagic vesicles, as well as by an activation of LC3-I into LC3-II leading to an enhancement of the [(LC3-II) / (LC3-I)] ratio (**Fig. 10**). Of note, DMF and MMF were able to counteract 7β-OHC-induced apoptosis and autophagy. Thus, in (7β-OHC + DMF)- and (7β-OHC + MMF)-treated cells, the percentage of apoptotic cells was strongly and significantly decreased, and the cleavage of caspase-3 was also reduced; in addition, the percentage of AO positive cells was also strongly decreased and the activation of LC3-I into LC3-II was diminished (**Fig. 10**). As little is known on the signaling pathway leading to 7β-OHC-induced cell death, various inhibitors were used: H89 (20 µM), U73122 (1 µM), chelerythrine (1 µM), and U0126 (20 µM), which inhibit protein kinase A (PKA), phospholipase C (PLC), protein kinase C (PKC) and

MEK, respectively. Undetectable or slight inhibition of cell death evaluated with the FDA assay was observed when 7β-OHC was associated with U73122 and H89, respectively (**Fig. 11**). However, 7β-OHC-induced cell death was markedly reduced in the presence of chelerythrine and U0126 (**Fig. 11**) supporting an involvement of PKC and MEK in the deleterious effects of 7β-OHC in 158N cells.

3.7. Effect of dimethyl fumarate and monomethyl fumarate on the recovery of 7β-hydroxycholesterol-induced cell death

We also studied the effect of DMF (25 µM) and MMF (25 µM) on 7β-OHC (50 µM)-induced cell death when DMF and MMF were added after 7β-OHC. With the FDA assay, the ability of α-tocopherol (400 µM) to prevent 7β-OHC-induced cell death was the most efficient when it was introduced in the culture medium 6 h after 7β-OHC; whereas significant, the cytoprotection found when α-tocopherol was introduced 10 h after 7β-OHC, was very slight (**Supplementary Fig. 5**). Based on these data, the effects of DMF and MMF were evaluated when they were added 6 h after 7β-OHC;of note, under these conditions, data obtained by cell counting with trypan blue, and nuclear staining with Hoechst 33342 show that DMF and MMF prevent 7β-OHC-induced cell death and apoptosis (**Fig. 12**). Therefore, DMF and MMF also have cytoprotective effects on 7β-OHC-induced cell death when they are added after this oxysterol.

3.8. Analysis of myelin proteins expression (PLP, MBP) in 7β-hydroxycholesterol-treated murine oligodendrocytes 158N without or with dimethyl fumarate and monomethyl fumarate

Myelin proteins such as proteolipid protein (PLP) and myelin basic protein (MBP) correspond to 50 and 30% of myelin proteins, respectively [30], and are expressed by 158N cells [29]. Therefore, we determined whether PLP and MBP expression was affected by 7β-OHC (50 µM), and the impact of DMF (25 µM), MMF (25 µM) and α-tocopherol (400 µM; used as cytoprotective agent) on these proteins.

Compared to control cells, PLP expression was either similar or slightly lower in vehicles-treated cells (**supplementary Fig. 6**); it was similar in, α-tocopherol-, DMF- and MMF-treated cells (**supplementary Fig. 6**). However, PLP expression was higher in 7β-OHC-, (7β-OHC + α-tocopherol)-, and (7β-OHC + MMF)-treated cells (**supplementary Fig. 6**). In the mouse, MBP is present under 2 major (around 18.5 and 14 kDa) and two minor (around 21.5 and 17 kDa) forms [60]. In 158N cells, the 21 kDa (minor form) and 18 kDa (major form) were easily detected (**supplementary Fig. 6**). Compared to control cells, MBP expression was enhanced by DMF (**supplementary Fig. 6**). MBP expression was also higher in 7β-OHC-, (7β-OHC + α-tocopherol), (7β-OHC + DMF), and (7β-OHC + MMF)-treated cells (**supplementary Fig. 6**). Thus, an increase in

the expression of PLP and MBP is observed with 7β-OHC; the increase in PLP is not corrected by α-tocopherol, and DMF but normalized with MMF; the increase in MBP observed with 7β-OHC is slightly and non significantly accentuated in the presence of α-tocopherol (**supplementary Fig. 6**). DMF is more efficient than MMF to reduce the overexpression of PLP, mainly the 18 kDa (**supplementary Fig. 6**).

Discussion

Oxidative stress and mitochondrial dysfunction are involved in numerous neurodegenerative diseases [61]. These dysfunctions favor lipid peroxidation leading to increased levels of 7-ketocholesterol (7KC) and 7β-OHC [7, 19]. These oxysterols are found at significantly elevated levels in the brain, CSF and / or plasma of patients with AD [3], MS [9] as well as in patients with X-linked adrenoleukodystrophy [20]**.** These modifications could play a critical role in the evolution of neurodegenerative diseases since these oxysterols are able to modify numerous cellular functions [3]. Indeed, it has been reported that 7β-OHC as well as 7KC, known as indicators of oxidative stress [62]**,** contribute to disruption of Redox homeostasis and are potent inducers of inflammation and cell death in different cell types of the CNS [3, 16]. This simultaneous induction of cell death associated with oxidative stress, and presenting apoptotic and autophagic criteria, has been described in oligodendrocytes and microglial cells treated with 7KC, 7β-OHC and 24S-hydroxycholesterol, and was defined as oxiapoptophagy [8]. To prevent neurodegenerative diseases associated with these molecules, it is therefore important to better know their signaling pathways to develop therapeutic strategies to oppose their deleterious effects. Currently, the ability of several molecules to attenuate oxysterols-induced oxiapoptophagy was mainly studied on oligodendrocytes 158N and the most powerful compound identified at the moment is α-tocopherol [8, 17, 19, 39]**.** In the present study, DMF and its main metabolite, MMF, have been chosen to counteract 7β-OHC-induced oxidative stress, mitochondrial damage and cell death given their ability to prevent oxidative stress via upregulation of anti-oxidative mechanisms [63]. DMF, marketed under the name of Tecfidera (Biogen), is used to treat the relapsing-remitting form of MS. In this study, 158N murine cells were used since they present several characteristics of differentiated oligodendrocytes, which are myelin producing cells in the CNS and consequenty essential for an efficient transmission of the nervous impulse. In addition, 158N cells express major myelin proteins (PLP, MBP) [29]. Therefore, the effects of 7β-OHC with or without DMF and MMF on PLP and MBP expression was also evaluated. Our data show important cytoprotective effects of DMF and MMF on 7β-OHC-treated 158N cells, and demonstrate the ability of DMF and MMF to prevent 7β-OHC-induced oxiapoptophagy.

In 158N cells, 7β-OHC exhibits cytotoxic effects. An increased percentage of floating round cells and a decreased of adherent cells associated with a loss of membrane integrity were revealed, suggesting an alteration of membrane constituents associated with cell death. These alterations could be explained by Redox disequilibrum induced by 7β-OHC, which could affect the different cellular compartments as a consequence of lipid peroxidation. Indeed, an overproduction of ROS and of mitochondrial $O_2^{\bullet -}$ associated with an enhancement of antioxidant enzyme activities (SOD, catalase, GPx), as well as lipid and protein oxidized derivatives were revealed under treatment with 7β-OHC. The enhanced activity of SOD evocates the data obtained by **Yuan et al.**, who showed that human macrophages exposed to 7KC have increased levels of MnSOD mRNA [50]. The increased levels of GPx, catalase, and SOD activities, were considered as a cellular reaction involved in the defense against the free radicals. The overproduction of ROS could favor the increase of SOD, catalase and GPx activities in a cascade of events to reduce oxidative stress. The disruption of Redox equilibrium observed under treatment with 7β-OHC, in agreement with previous studies [8, 19, 34, 64], is also associated with an increase of lipid and protein oxidation (MDA, CDs and CPs) which could be used as biomarkers of oxidative stress in diseases associated with increased levels of this oxysterol.

In 158N cells exposed to 7β-OHC, as observed under treatment with 7KC [39], the overproduction of ROS was associated with a loss of transmembrane mitochondrial potential (ΔΨm). Thus, we were interested in the characterization of mitochondrial functions in the presence of 7β-OHC. In agreement with previous studies, we found that 7β-OHC is an inducer of cell death associated with mitochondrial dysfunction, including morphological, functional and metabolic mitochondrial alterations [8]. This includes: a loss of succinate dehydrogenase activity, a loss of ΔΨm, an increase of mitochondrial mass, and an overproduction of $O_2^{\bullet -}$ at the mitochondria level. These findings are in accordance with studies conducted on various cell types from different species [16, 17]. The increase of mitochondrial mass could be an adaptative response of the mitochondria to prevent the loss of transmembrane mitochondrial potential and preserve mitochondrial metabolism [65]. It has been reported that an increase of mitochondrial mass was correlated to the hyperactivity of the mitochondrial complex IV in the axons of patients with MS [66, 67]. As it is known, the main mitochondrial function is to control respiratory chain in order to produce energy in the form of ATP via TCA cycle which is primordial for numerous cellular functions such as carbohydrates, proteins and lipids metabolism [68]. Here, we remarked an enhancement of cellular lactate (lactic acid), associated with a decrease of pyruvate level in the presence of 7β-OHC. This suggests a defect of carbohydrate metabolism and in particular of glycolysis. The accumulation of lactic acid could result from pyruvate conversion to regenerate NAD^+ used to restore glycolysis. Since pyruvate is the precursor of acetyl-CoA, the decreased amount of pyruvate could be at the origin of TCA cycle impairment. The alteration of the TCA cycle is supported

764 by the reduced concentrations of some organic acids of the TCA cycle, citrate, fumarate, succinate, and
765 malate in the presence of 7β-OHC. TCA cycle impairment can lead to oxidative phosphorylation
766 alteration, and consequently to mitochondrial failure [39]. On the other hand, 7β-OHC induces a
767 decrease in the cardiolipin levels. Similar observations were made in158N exposed to 7KC [69].
768 Cardiolipins are mitochondrial phospholipids synthesized and located in the inner mitochondrial
769 membrane, and are involved in various mitochondrial functions and in bioenergetics [58]. The loss of
770 cardiolipin content in mitochondria may also reflect biochemical modifications of mitochondrial
771 membrane. It is suggested that the observed decrease of cardiolipin content could be consequence of
772 their increased hydrolysis by endogenous phospholipases, and/or by a decreased de novo synthesis
773 resulting from impaired function of the enzymes involved in their synthesis, or by a decreased
774 bioavailability of cardiolipin precursors. During cell death, release of cardiolipins outside the
775 mitochondria and outside the cells is also possible. These data underline the major role of 7β-OHC in
776 mitochondrial dysfunction.
777 Given the important role of lipids, including cholesterol in myelin structure and brain health [70], it
778 was important to evaluate the impact of 7β-OHC on cholesterol metabolism via the quantification of
779 some of its precursors and derivatives. Under treatment with 7β-OHC, reduced levels of total
780 cholesterol and its precursors, lathosterol, lanosterol, and desmosterol were observed, arguing in favor
781 a defect on cholesterol synthesis. Our results support previous findings reported on different cellular
782 lines treated with 24(S)-hydroxycholesterol or 7KC: these studies have shown that cholesterol
783 synthesis alteration was associated with other events such as mitochondrial damage and cell death
784 [39]. As our study reveals oxidative stress along with severe mitochondrial dysfunctions, under
785 treatment with 7β-OHC, this could explain even in part, the cellular accumulation of 7KC formed by
786 an oxidation of cholesterol induced by ROS overproduction.
787 Our results support the idea that the alteration of cholesterol synthesis, lead to cholesterol homeostasis
788 disturbance, which in oxidative stress conditions might be associated with increased levels of some
789 oxysterols. In addition, it has been reported that oxysterols can disturb lipid homeostasis through the
790 activation of transcription factors. They can act on sterol responsive element binding proteins
791 (SREBPs), which activate several genes involved in cholesterol, triglycerides, phospholipids, and fatty
792 acid synthesis [71]. In addition, fatty acids, which are components of phospholipids, are essential
793 constituents in the structure and functions of myelin sheath [72]. Thus, it was important to evaluate
794 both the fatty acid profile and the phospholipid content (sphingomyelin, phosphatidylcholine) when
795 158N cells were exposed to 7β-OHC. In this condition, a reduction of saturated fatty acids as myristic
796 acid (C14:0), palmitic acid (C16:0) and stearic acid (C18:0), structural elements of membrane
797 phospholipids, as well as of phosphatidylcholine and sphingomyelin were observed. In addition, an

accumulation of total and very long chain saturated fatty acids (VLCSFAs) has been remarked under treatment with 7β-OHC, which points towards peroxisomal defect, since β-oxidation of VLCSFAs leading to their degradation takes place in the peroxisome [73]. Thus, as reported with 7KC, the treatment with 7β-OHC also induces peroxisomal dysfunction [69]. Furthermore, it has been demonstrated that the VLCSFAs are able to induce cell death, mitochondrial impairment, and oxidative stress in nerve cells [74], which could aggravate the cytotoxic effect of 7β-OHC. Moreover, MUFA and PUFA levels were also reduced, which is in accordance with other studies, conducted on 158N cells in the presence of 7β-OHC [34]. It is also well established that MUFA and PUFA are indispensable for neuronal membrane fluidity [75], and have neuroprotective, anti-inflammatory, and antioxidant properties [76, 77].

According to previous findings on different cell lines, 7β-OHC was considered as a strongly cytotoxic oxysterol. So, we intended to characterize 7β-OHC-induced cell death. Our data show that 7β-OHC-induced cell death triggers caspase-3 activation associated with fragmented and/or condensed nuclei. This supports that 7β-OHC induces an apoptotic mode of cell death. Moreover, our data confirm that 7β-OHC also triggers autophagy. Indeed, a higher percentage of cells with altered lysosomes was observed. These data underline that 7β-OHC-induced cell death is characterized by lysosomal dysfunction [78] which could favour mitochondrial alteration [79]. Furthermore, a conversion of LC3-I to LC3-II, and an increase of (LC3-II / LC3-I) ratio, which are characteristics of autophagy, were detected demonstrating that 7β-OHC simultaneously triggers apoptosis and autophagy, and induces an oxiapoptophagic process [64]. Altogether, our data highlight the major role played by 7β-OHC in mitochondrial dysfunction, oxidative stress induction, cellular metabolism alteration and cell death induction which are common features observed during neurodegeneration. In addition, our study brings new information on the signalling pathway induced during 7β-OHC-induced cell death and supports the hypothesis of an activation of the PKC / p38 / MEK signalling pathway [18].

When 158N cells were simultaneously treated with DMF or MMF and 7β-OHC, our data demonstrate that DMF, a therapeutic agent (prescribed under the name of Tecfidera used for the treatment of relapsing remitting MS), as well as MMF, which is its major metabolite, known to have antioxidant and neuroprotective activities are able to prevent 7β-OHC-induced cytotoxicity [22, 23]. Under these conditions, we observed an attenuation of cell detachment and a preservation of plasma membrane integrity. It has also been shown that DMF induces an increase of antioxidant molecules such as glutathione (GSH), carnitine, and ascorbic acid above basal levels [24]. These molecules, especially ascorbic acid, are able to maintain membrane integrity in a pro-oxidative environment by preventing lipid peroxidation [80]. In our study, the ability of DMF to increase the levels of SH-groups suggests that this compound might favor this mechanism. It may act through the activation of Nrf2 pathway

[81]. Thus, it was of interest to evaluate the part taken by DMF and its major metabolite MMF on Redox status. We therefore determine the ability of DMF and MMF to inhibit the overproduction of ROS, to increase the antioxidant enzyme activities (SOD, catalase, GPx), to increase SH-groups level, and to reduce lipid peroxidation and protein oxidation products. Overall, the cytotoxic effects induced by 7β-OHC on 158N cells were strongly attenuated by DMF and MMF. In line with these findings, on human oligodendrocytes (MO3.13 cells), it has been reported that DMF prevent H_2O_2 overproduction-induced cell death, and enhances antioxidant molecule levels [24]. In the presence of 7β-OHC, treatment with DMF and MMF favors the recovery of mitochondrial function through the restoration of succinate dehydrogenase activity, and mitochondrial transmembrane potential. Furthermore, DMF and MMF are able to counteract mitochondrial $O_2^{\bullet-}$ overproduction, supporting a role of DMF and MMF on the control of cellular Redox potential [82]. In addition, DMF and MMF were able to attenuate the increase of mitochondrial mass corresponding either to an increase of the number of mitochondria and/or of their size [34]. Moreover, DMF and MMF normalize cardiolipin levels. Since a loss of cardiolipin content or alterations in the composition of these molecules have been associated with mitochondrial dysfunction, the restoration of their content argues in favor of the ability of DMF and MMF to prevent and restore mitochondrial dysfunction. This conclusion is reinforced by the ability of DMF and MMF to prevent TCA cycle alterations. These results underline that DMF and MMF influence the activities of mitochondrial enzymes including those of the TCA cycle. Pyruvate levels were also increased associated with a reduction of lactate after preatreatment with DMF or MMF: this argues in favour a recovery on carbohydrate metabolism and especially glycolysis.

It is also well known that the myelin sheath is composed of approximately 70–80% of lipids [72]. The synthesis and incorporation of phospholipids, sphingolipids, and cholesterol are critical for its development and maintenance. Based on data demonstrating neuroprotection of DMF, we postulated that this molecule and its metabolite (MMF) might increase the synthesis of lipids, which are major components of myelin sheath. Of note, DMF and MMF were able to prevent 7β-OHC-induced modification of cholesterol synthesis through the restoration of the content of cholesterol precursors. The formation of oxidized cholesterol derivatives (mainly 7KC) resulting chiefly from cholesterol autoxidation was also reduced in the presence of DMF or MMF. However, DMF and MMF were unable to prevent the intracellular accumulation of 7β-OHC. As the expression of the gene HSD11B1 encoding for the enzyme 11β-HSD1 is considered unlikely, a conversion of 7β-OHC to 7KC by this enzyme, is excluded. On the other hand, as the gene HSD11B2 encoding for the enzyme 11β-HSD2 catalyzing the conversion of 7β-OHC to 7KC is expressed, this may explain the persistent presence of 7KC despite the powerful antioxidant effects of DMF and MMF. In addition, we report the ability of DMF and MMF to normalize the fatty acid profile. The reduction of VLCSFAs levels observed when

7β-OHC was associated with DMF and MMF support that DMF and MMF not only tend to normalize mitochondrial activity, but also peroxisomal activity.Of note, DMF and MMF were also able to attenuate the decrease of phospholipids (sphingomyelin, phosphatidylcholine) which are important component of myelin. Indeed, whereas the molar ratio of cholesterol, phospholipids and glycosphingolipids in most membranes is in the order of 25%:65%:10%, the molar ratios in myelin are in the range of 40%:40%:20% [83]. As DMF and MMF contribute to restore a normal lipid profile, concerning myelin associated-lipids (cholesterol, phospholipids), it was important to determine how major myelin proteins such as proteolipid protein (PLP) and myelin basic protein (MBP), which correspond to 50 and 30% of myelin proteins, respectively [30], and which are expressed by the 158N cells [29], were affected by 7β-OHC and what was the impact of DMF and MMF on these proteins. Noteworthy, the increased expression of PLP was normalized with MMF, and the increase expression of MBP observed with 7β-OHC was more or less attenuated by DMF and MMF.

Finally, DMF and MMF are also able to counteract 7β-OHC-induced apoptosis as well as autophagy. At the moment, on 158N cells, similar cytoprotective effects were only observed with α-tocopherol, DHA, and biotin which allow attenuation of 7β-OHC-induced oxiapoptophagy [8, 31].

Conclusion

Our data obtained on oligodendrocytes 158N demonstrate that 7β-OHC induces ROS overproduction subsequently leading to increased antioxidant enzyme activity, and oxidation of cellular macromolecules. In addition, 7β-OHC triggers important mitochondrial dysfunctions: decreases of $\Delta\Psi m$, increases of mitochondrial mass, decreased cardiolipin content and alteration of the TCA cycle, which can influence the cellular metabolism, especially lipid metabolism. These different alterations contribute to cell death through oxiapoptophagy. The different events associated with oxiapoptophagy, revealed from data obtained in the present study and in previous studies, are summarized in **Supplementary Fig. 7**. Our data also show that DMF and MMF attenuate 7β-OHC-induced oxidative stress, mitochondrial dysfunction, lipid metabolism alteration and cell death, which are hallmarks of neurodegenerative diseases. As 7β-OHC is associated with neurodegeneration, the ability of DMF and MMF to counteract the toxicity of this oxysterol reinforces the interest of DMF for the treatment of neurodegenerative diseases as well as of other diseases associated with increased levels of 7β-OHC [3, 16].

Conflict of interest: The authors have no conflict of interest to declare.

Acknowledgments: This work was presented as a poster at the 8th ENOR Symposium "Oxysterols and Sterols: from Lipidomics to Food Sciences", September 20–21, 2018, University of Bologna, Bologna, Italy (https://www.oxysterols.net/). This work was supported by grants from: Univ. Bourgogne (Dijon, France), Univ. Monastir (Monastir, Tunisia), and Univ. Manouba (Tunis, Tunisia). We acknowledge Dr Delphine Meffre (Inserm UMR 1124, Paris, France) for her valuable advice on the choice of anti-PLP and and anti-MBP antibodies, and for the conditions of analysis of these proteins by Western blotting.

References

[1] D.J., Betteridge. What is oxidative stress? Metabolism. 49(2 Suppl 1)(2000)3-8.

[2] L.M. Sayre, G. Perry, M.A. Smith, Oxidative stress and neurotoxicity, Chemical research in toxicology, 21 (2007) 172-188.

[3] A. Zarrouk, A. Vejux, J. Mackrill, Y. O'Callaghan, M. Hammami, N. O'Brien, G. Lizard, Involvement of oxysterols in age-related diseases and ageing processes, Ageing research reviews, 18 (2014) 148-162.

[4] M.T. Fischer, R. Sharma, J.L. Lim, L. Haider, J.M. Frischer, J. Drexhage, D. Mahad, M. Bradl, J. van Horssen, H. Lassmann, NADPH oxidase expression in active multiple sclerosis lesions in relation to oxidative tissue damage and mitochondrial injury, Brain, 135 (2012) 886-899.

[5] G.R. Campbell, D.J. Mahad, Mitochondria as crucial players in demyelinated axons: lessons from neuropathology and experimental demyelination, Autoimmune diseases, 2011 (2011).

[6] A. Zarrouk, M. Debbabi, M. Bezine, E.M. Karym, A. Badreddine, O. Rouaud, T. Moreau, M. Cherkaoui-Malki, M. El Ayeb, B. Nasser, Lipid Biomarkers in Alzheimer's Disease, Current Alzheimer Research, 15 (2018) 303-312.

[7] L. Iuliano, Pathways of cholesterol oxidation via non-enzymatic mechanisms, Chemistry and physics of lipids, 164 (2011) 457-468.

[8] T. Nury, A. Zarrouk, J.J. Mackrill, M. Samadi, P. Durand, J.-M. Riedinger, M. Doria, A. Vejux, E. Limagne, D. Delmas, Induction of oxiapoptophagy on 158N murine oligodendrocytes treated by 7-ketocholesterol-, 7β-hydroxycholesterol-, or 24 (S)-hydroxycholesterol: Protective effects of α-tocopherol and docosahexaenoic acid (DHA; C22: 6 n-3), Steroids, 99 (2015) 194-203.

[9] V. Leoni, D. Lütjohann, T. Masterman, Levels of 7-oxocholesterol in cerebrospinal fluid are more than one thousand times lower than reported in multiple sclerosis, Journal of lipid research, 46 (2005) 191-195.

[10] M. Doria, L. Maugest, T. Moreau, G. Lizard, A. Vejux, Contribution of cholesterol and oxysterols to the pathophysiology of Parkinson's disease, Free Radical Biology and Medicine, 101 (2016) 393-400.

[11] F. Kreilaus, A.S. Spiro, C.A. McLean, B. Garner, A.M. Jenner, Evidence for altered cholesterol metabolism in H untington's disease post mortem brain tissue, Neuropathology and applied neurobiology, 42 (2016) 535-546.

933 **[12]** G. Testa, E. Staurenghi, C. Zerbinati, S. Gargiulo, L. Iuliano, G. Giaccone, F. Fantò, G. Poli, G. Leonarduzzi, P.
934 Gamba, Changes in brain oxysterols at different stages of Alzheimer's disease: Their involvement in
935 neuroinflammation, Redox biology, 10 (2016) 24-33.
936 **[13]** T.J. Nelson, D.L. Alkon, Oxidation of cholesterol by amyloid precursor protein and β-amyloid peptide,
937 Journal of Biological Chemistry, 280 (2005) 7377-7387.
938 **[14]** H. Larsson, Y. Böttiger, L. Iuliano, U. Diczfalusy, In vivo interconversion of 7β-hydroxycholesterol and 7-
939 ketocholesterol, potential surrogate markers for oxidative stress, Free Radical Biology and Medicine, 43 (2007)
940 695-701.
941 **[15]** A. Odermatt, P. Klusonova, 11β-Hydroxysteroid dehydrogenase 1: Regeneration of active glucocorticoids
942 is only part of the story, The Journal of steroid biochemistry and molecular biology, 151 (2015) 85-92.
943 **[16]** A. Vejux, G. Lizard, Cytotoxic effects of oxysterols associated with human diseases: Induction of cell death
944 (apoptosis and/or oncosis), oxidative and inflammatory activities, and phospholipidosis, Molecular aspects of
945 medicine, 30 (2009) 153-170.
946 **[17]** A. Zarrouk, T. Nury, M. Samadi, Y. O'Callaghan, M. Hammami, N.M. O'Brien, G. Lizard, J.J. Mackrill, Effects
947 of cholesterol oxides on cell death induction and calcium increase in human neuronal cells (SK-N-BE) and
948 evaluation of the protective effects of docosahexaenoic acid (DHA; C22: 6 n-3), Steroids, 99 (2015) 238-247.
949 **[18]** L. Clarion, M. Schindler, J. de Weille, K. Lolmède, A. Laroche-Clary, E. Uro-Coste, J. Robert, M. Mersel, N.
950 Bakalara, 7β-Hydroxycholesterol-induced energy stress leads to sequential opposing signaling responses and
951 to death of C6 glioblastoma cells, Biochemical pharmacology, 83 (2012) 37-46.
952 **[19]** K. Ragot, J.J. Mackrill, A. Zarrouk, T. Nury, V. Aires, A. Jacquin, A. Athias, J.-P.P. de Barros, A. Véjux, J.-M.
953 Riedinger, Absence of correlation between oxysterol accumulation in lipid raft microdomains, calcium
954 increase, and apoptosis induction on 158N murine oligodendrocytes, Biochemical pharmacology, 86 (2013) 67-
955 79.
956 **[20]** T. Nury, A. Zarrouk, K. Ragot, M. Debbabi, J.-M. Riedinger, A. Vejux, P. Aubourg, G. Lizard, 7-
957 Ketocholesterol is increased in the plasma of X-ALD patients and induces peroxisomal modifications in
958 microglial cells: Potential roles of 7-ketocholesterol in the pathophysiology of X-ALD, The Journal of steroid
959 biochemistry and molecular biology, 169 (2017) 123-136.
960 **[21]** D. Werdenberg, R. Joshi, S. Wolffram, H.P. Merkle, P. Langguth, Presystemic metabolism and intestinal
961 absorption of antipsoriatic fumaric acid esters, Biopharmaceutics & drug disposition, 24 (2003) 259-273.
962 **[22]** S.X. Lin, L. Lisi, C.D. Russo, P.E. Polak, A. Sharp, G. Weinberg, S. Kalinin, D.L. Feinstein, The anti-
963 inflammatory effects of dimethyl fumarate in astrocytes involve glutathione and haem oxygenase-1, ASN
964 neuro, 3 (2011) AN20100033.
965 **[23]** R.H. Scannevin, S. Chollate, M.-y. Jung, M. Shackett, H. Patel, P. Bista, W. Zeng, S. Ryan, M. Yamamoto, M.
966 Lukashev, Fumarates promote cytoprotection of central nervous system cells against oxidative stress via the

nuclear factor (erythroid-derived 2)-like 2 pathway, Journal of Pharmacology and Experimental Therapeutics, 341 (2012) 274-284.

[24] H. Huang, A. Taraboletti, L.P. Shriver, Dimethyl fumarate modulates antioxidant and lipid metabolism in oligodendrocytes, Redox biology, 5 (2015) 169-175.

[25] E. Havrdova, M. Hutchinson, N.C. Kurukulasuriya, K. Raghupathi, M.T. Sweetser, K.T. Dawson, R. Gold, Oral BG-12 (dimethyl fumarate) for relapsing–remitting multiple sclerosis: a review of DEFINE and CONFIRM: Evaluation of: Gold R, Kappos L, Arnold D, et al. Placebo-controlled phase 3 study of oral BG-12 for relapsing multiple sclerosis. N Engl J Med 2012; 367: 1098-107; and Fox RJ, Miller DH, Phillips JT, et al. Placebo-controlled phase 3 study of oral BG-12 or glatiramer in multiple sclerosis. N Engl J Med 2012; 367: 1087-97, Expert opinion on pharmacotherapy, 14 (2013) 2145-2156.

[26] Z. Xu, F. Zhang, F. Sun, K. Gu, S. Dong, D. He, Dimethyl fumarate for multiple sclerosis, Cochrane Data Base Syst Rev 4 (2015) CDO 11076.

[27] G.O. Gillard, B. Collette, J. Anderson, J. Chao, R.H. Scannevin, D.J. Huss, J.D. Fontenot, DMF, but not other fumarates, inhibits NF-κB activity in vitro in an Nrf2-independent manner, Journal of neuroimmunology, 283 (2015) 74-85.

[28] R.A. Linker, D.-H. Lee, S. Ryan, A.M. van Dam, R. Conrad, P. Bista, W. Zeng, X. Hronowsky, A. Buko, S. Chollate, Fumaric acid esters exert neuroprotective effects in neuroinflammation via activation of the Nrf2 antioxidant pathway, Brain, 134 (2011) 678-692.

[29] M. Baarine, K. Ragot, EC Genin, H El Hajj, D Trompier, P Andreoletti, MS Ghandour, F Menetrier, M Cherkaoui-Malki, S Savary, G Lizard. Peroxisomal and mitochondrial status of two murine oligodendrocytic cell lines (158N, 158JP): potential models for the study of peroxisomal disorders associated with dysmyelination processes. J Neurochem. 111(1) (2009) 119-31.

[30] N Baumann, D Pham-Dinh. Biology of oligodendrocyte and myelin in the mammalian central nervous system. Physiol Rev. 81(2) (2001) 871-927.

[31] R Sghaier, A Zarrouk, T Nury, B Ilham, N O'Brien, JJ Mackrill, A Vejux, M Samadi, B Nasser, C Caccia, V Leoni, T Moreau, M Cherkaoui-Malki, A Salhedine Masmoudi, G Lizard. Biotin attenuation of oxidative stress, mitochondrial dysfunction, lipid metabolism alteration and 7β-hydroxycholesterol-induced cell death in 158N murine oligodendrocytes. Free Radic Res. 2019 May 1:1-11. doi: 10.1080/10715762.2019.1612891

[32] K.H. Jones, J.A. Senft, An improved method to determine cell viability by simultaneous staining with fluorescein diacetate-propidium iodide, Journal of Histochemistry & Cytochemistry, 33 (1985) 77-79.

[33] G. Lizard, S. Fournel, L. Genestier, N. Dhedin, C. Chaput, M. Flacher, M. Mutin, G. Panaye, J.P. Revillard, Kinetics of plasma membrane and mitochondrial alterations in cells undergoing apoptosis, Cytometry Part A, 21 (1995) 275-283.

[34] A. Zarrouk, Y.B. Salem, J. Hafsa, R. Sghaier, B. Charfeddine, K. Limem, M. Hammami, H. Majdoub, 7β-hydroxycholesterol-induced cell death, oxidative stress, and fatty acid metabolism dysfunctions attenuated with sea urchin egg oil, Biochimie, 153 (2018) 201-219.

[35] A. Zarrouk, T. Nury, E.-M. Karym, A. Vejux, R. Sghaier, C. Gondcaille, P. Andreoletti, D. Trompier, S. Savary, M. Cherkaoui-Malki, Attenuation of 7-ketocholesterol-induced overproduction of reactive oxygen species, apoptosis, and autophagy by dimethyl fumarate on 158N murine oligodendrocytes, The Journal of steroid biochemistry and molecular biology, 169 (2017) 29-38.

[36] A. Zarrouk, A. Vejux, T. Nury, H.I. El Hajj, M. Haddad, M. Cherkaoui-Malki, J.-M. Riedinger, M. Hammami, G. Lizard, Induction of mitochondrial changes associated with oxidative stress on very long chain fatty acids (C22: 0, C24: 0, or C26: 0)-treated human neuronal cells (SK-NB-E), Oxidative medicine and cellular longevity, 2012 (2012).

[37] J. Folch, M. Lees, G. Sloane-Stanley, A simple method for the isolation and purification of total lipids from animal tissues, J biol Chem, 226 (1957) 497-509.

[38] G. Vial, M.-A. Chauvin, N. Bendridi, A. Durand, E. Meugnier, A.-M. Madec, N. Bernoud-Hubac, J.-P.P. de Barros, É. Fontaine, C. Acquaviva, Imeglimin normalizes glucose tolerance and insulin sensitivity and improves mitochondrial function in liver of a high-fat high-sucrose diet mice model, Diabetes, (2015) db141220.

[39] V. Leoni, T. Nury, A. Vejux, A. Zarrouk, C. Caccia, M. Debbabi, A. Fromont, R. Sghaier, T. Moreau, G. Lizard, Mitochondrial dysfunctions in 7-ketocholesterol-treated 158N oligodendrocytes without or with α-tocopherol: Impacts on the cellular profil of tricarboxylic cycle-associated organic acids, long chain saturated and unsaturated fatty acids, oxysterols, cholesterol and cholesterol precursors, The Journal of steroid biochemistry and molecular biology, 169 (2017) 96-110.

[40] V. Leoni, L. Strittmatter, G. Zorzi, F. Zibordi, S. Dusi, B. Garavaglia, P. Venco, C. Caccia, A.L. Souza, A. Deik, Metabolic consequences of mitochondrial coenzyme A deficiency in patients with PANK2 mutations, Molecular genetics and metabolism, 105 (2012) 463-471.

[41] L. Flohé, W.A. Günzler, [12] Assays of glutathione peroxidase, Methods in enzymology, 105 (1984) 114-120.

[42] H.P. Misra, I. Fridovich, The role of superoxide anion in the autoxidation of epinephrine and a simple assay for superoxide dismutase, Journal of Biological chemistry, 247 (1972) 3170-3175.

[43] P. Faure, J.-L. Lafond, Measurement of plasma sulfhydryl and carbonyl groups as a possible indicator of protein oxidation, Analysis of free radicals in biological systems, Springer1995, pp. 237-248.

[44] G. Rothe, G. Valet, Flow cytometric analysis of respiratory burst activity in phagocytes with hydroethidine and 2', 7'-dichlorofluorescin, Journal of leukocyte biology, 47 (1990) 440-448.

[45] G. Rothe, A. Oser, G. Valet, Dihydrorhodamine 123: a new flow cytometric indicator for respiratory burst activity in neutrophil granulocytes, Naturwissenschaften, 75 (1988) 354-355.

[46] H. Esterbauer, G. Striegl, H. Puhl, M. Rotheneder, Continuous monitoring of in vztro oxidation of human low density lipoprotein, Free radical research communications, 6 (1989) 67-75.

[47] T. Yoshioka, K. Kawada, T. Shimada, M. Mori, Lipid peroxidation in maternal and cord blood and protective mechanism against activated-oxygen toxicity in the blood, American journal of obstetrics and gynecology, 135 (1979) 372-376.

[48] C.N. Oliver, B.-W. Ahn, E.J. Moerman, S. Goldstein, E.R. Stadtman, Age-related changes in oxidized proteins, Journal of Biological Chemistry, 262 (1987) 5488-5491.

[49] M. Baarine, K. Ragot, A. Athias, T. Nury, Z. Kattan, E.C. Genin, P. Andreoletti, F. Ménétrier, J.-M. Riedinger, M. Bardou, Incidence of Abcd1 level on the induction of cell death and organelle dysfunctions triggered by very long chain fatty acids and TNF-α on oligodendrocytes and astrocytes, Neurotoxicology, 33 (2012) 212-228.

[50] X.M. Yuan, W. Li, U.T. Brunk, H. Dalen, Y.H. Chang, A. Sevanian, Lysosomal destabilization during macrophage damage induced by cholesterol oxidation products, Free Radical Biology and Medicine, 28 (2000) 208-218.

[51] M. Olsson, I. Rundquist, U. Brunk, Flow cytofluorometry of lysosomal acridine orange uptake by living cultured cells effect of trypsinization and starvation, Acta Pathologica Microbiologica Scandinavica Series A: Pathology, 95 (1987) 159-165.

[52] A. Altmeyer, A.C. Jung, M. Ignat, S. Benzina, J.-M. Denis, J. Gueulette, G. Noel, D. Mutter, P. Bischoff, Pharmacological enhancement of autophagy induced in a hepatocellular carcinoma cell line by high-LET radiation, Anticancer research, 30 (2010) 303-310.

[53] AH Kilgour, S Semple, I Marshall, P Andrews, R Andrew, BR Walker. 11β-Hydroxysteroid dehydrogenase activity in the brain does not contribute to systemic interconversion of cortisol and cortisone in healthy men. J Clin Endocrinol Metab. 100(2) (2015) 483-9. doi: 10.1210/jc.2014-3277.

[54] M Wamil, R Andrew, KE Chapman, J Street, NM Morton, JR Seckl. 7-oxysterols modulate glucocorticoid activity in adipocytes through competition for 11beta-hydroxysteroid dehydrogenase type. Endocrinology. 149(12) (2008) 5909-18. doi: 10.1210/en.2008-0420.

[55] T Mitić, S Shave, N Semjonous, I McNae, DF Cobice, GG Lavery, SP Webster, PW Hadoke, BR Walker, R Andrew. 11β-Hydroxysteroid dehydrogenase type 1 contributes to the balance between 7-keto- and 7-hydroxy-oxysterols in vivo. Biochem Pharmacol. 86(1) (2013) 146-53. doi: 10.1016/j.bcp.2013.02.002.

[**56**] WJ Griffiths, Y Wang. Oxysterol research: a brief review. Biochem Soc Trans. 47(2)(2019)517-526.

[57] A. Birk, W. Chao, C. Bracken, J. Warren, H. Szeto, Targeting mitochondrial cardiolipin and the cytochrome c/cardiolipin complex to promote electron transport and optimize mitochondrial ATP synthesis, British journal of pharmacology, 171 (2014) 2017-2028.

[58] G. Paradies, V. Paradies, V. De Benedictis, F.M. Ruggiero, G. Petrosillo, Functional role of cardiolipin in mitochondrial bioenergetics, Biochimica et Biophysica Acta (BBA)-Bioenergetics, 1837 (2014) 408-417.

[59] M. Schrader, J. Costello, L.F. Godinho, M. Islinger, Peroxisome-mitochondria interplay and disease, Journal of inherited metabolic disease, 38 (2015) 681-702.

[60] AT Campagnoni, B Sorg, HJ Roth, K Kronquist, SL Newman, K Kitamura, C Campagnoni, B Crandall, Expression of myelin protein genes in the developing brain. J Physiol (Paris). 82(4) (1987) 229-238.

[61] M. Di Carlo, D. Giacomazza, P. Picone, D. Nuzzo, P.L. San Biagio, Are oxidative stress and mitochondrial dysfunction the key players in the neurodegenerative diseases?, Free radical research, 46 (2012) 1327-1338.

[62] B. Ziedén, A. Kaminskas, M. Kristenson, Z. Kucinskienê, B. Vessby, A.G. Olsson, U. Diczfalusy, Increased plasma 7β-hydroxycholesterol concentrations in a population with a high risk for cardiovascular disease, Arteriosclerosis, thrombosis, and vascular biology, 19 (1999) 967-971.

[63] R.J. Fox, M. Kita, S.L. Cohan, L.J. Henson, J. Zambrano, R.H. Scannevin, J. O'Gorman, M. Novas, K.T. Dawson, J.T. Phillips, BG-12 (dimethyl fumarate): a review of mechanism of action, efficacy, and safety, Current medical research and opinion, 30 (2014) 251-262.

[64] T. Nury, M. Samadi, A. Zarrouk, J.M. Riedinger, G. Lizard, Improved synthesis and in vitro evaluation of the cytotoxic profile of oxysterols oxidized at C4 (4α-and 4β-hydroxycholesterol) and C7 (7-ketocholesterol, 7α-and 7β-hydroxycholesterol) on cells of the central nervous system, European journal of medicinal chemistry, 70 (2013) 558-567.

[65] J.M. Zahm, S. Baconnais, S. Monier, N. Bonnet, G. Bessède, P. Gambert, E. Puchelle, G. Lizard, Chronology of cellular alterations during 7-ketocholesterol–induced cell death on A7R5 rat smooth muscle cells: Analysis by time lapse-video microscopy and conventional fluorescence microscopy, Cytometry Part A: The Journal of the International Society for Analytical Cytology, 52 (2003) 57-69.

[66] D.J. Mahad, I. Ziabreva, G. Campbell, N. Lax, K. White, P.S. Hanson, H. Lassmann, D.M. Turnbull, Mitochondrial changes within axons in multiple sclerosis, Brain, 132 (2009) 1161-1174.

[67] M.E. Witte, L. Bø, R.J. Rodenburg, J.A. Belien, R. Musters, T. Hazes, L.T. Wintjes, J.A. Smeitink, J.J.G. Geurts, H.E. De Vries, Enhanced number and activity of mitochondria in multiple sclerosis lesions, The Journal of Pathology: A Journal of the Pathological Society of Great Britain and Ireland, 219 (2009) 193-204.

[68] F. Pierrel, P.A. Cobine, D.R. Winge, Metal Ion availability in mitochondria, Biometals, 20 (2007) 675.

[69] T. Nury, R. Sghaier, A. Zarrouk, F. Ménétrier, T. Uzun, V. Leoni, C. Caccia, W. Meddeb, A. Namsi, K. Sassi, Induction of peroxisomal changes in oligodendrocytes treated with 7-ketocholesterol: Attenuation by α-tocopherol, Biochimie, 153 (2018) 151-202.

[70] J. Diestschy, S. Turley, Cholesterol metabolism in the central nervous system during early development and in the mature animal, J Lipid Res, 45 (2004) 1375-1397.

[71] J.D. Horton, J.L. Goldstein, M.S. Brown, SREBPs: activators of the complete program of cholesterol and fatty acid synthesis in the liver, The Journal of clinical investigation, 109 (2002) 1125-1131.

[72] P. Morell, R.H. Quarles, Characteristic composition of myelin, Basic neurochemistry: molecular, cellular and medical aspects, 6 (1999).

[73] R.J.A. Wanders, H.R. Waterham, Biochemistry of mammalian peroxisomes revisited, Annu. Rev. Biochem., 75 (2006) 295-332.

[74] I. Hapala, E. Marza, T. Ferreira, Is fat so bad? Modulation of endoplasmic reticulum stress by lipid droplet formation, Biology of the Cell, 103 (2011) 271-285.

[75] A.P. Simopoulos, Essential fatty acids in health and chronic disease, The American journal of clinical nutrition, 70 (1999) 560s-569s.

[76] C. Colette, C. Percheron, N. Pares-Herbute, F. Michel, T.C. Pham, L. Brillant, B. Descomps, L. Monnier, Exchanging carbohydrates for monounsaturated fats in energy-restricted diets: effects on metabolic profile and other cardiovascular risk factors, International journal of obesity, 27 (2003) 648.

[77] S.C. Dyall, Long-chain omega-3 fatty acids and the brain: a review of the independent and shared effects of EPA, DPA and DHA, Frontiers in aging neuroscience, 7 (2015).

[78] L. Malvitte, T. Montange, A. Vejux, C. Joffre, A. Bron, C. Creuzot-Garcher, G. Lizard, Activation of a Caspase-3-Independent Mode of Cell Death Associated with Lysosomal Destabilization in Cultured Human Retinal Pigment Epithelial Cells (ARPE-19) Exposed to 7β-Hydroxycholesterol, Current eye research, 33 (2008) 769-781.

[79] C.E. Chwieralski, T. Welte, F. Bühling, Cathepsin-regulated apoptosis, Apoptosis, 11 (2006) 143-149.

[80] G.R. Buettner, The pecking order of free radicals and antioxidants: lipid peroxidation, α-tocopherol, and ascorbate, Archives of biochemistry and biophysics, 300 (1993) 535-543.

[81] T. Nguyen, P. Nioi, C.B. Pickett, The Nrf2-antioxidant response element signaling pathway and its activation by oxidative stress, Journal of Biological Chemistry, 284 (2009) 13291-13295.

[82] A. Suneetha, Role of dimethyl fumarate in oxidative stress of multiple sclerosis: A review, Journal of Chromatography B, 1019 (2016) 15-20.

[83] J.S., O'Brien. Stability of the myelin membrane. Science. 147(1965) 1099-107.

[84] C Prunet, S Lemaire-Ewing, F Ménétrier, D Néel, G Lizard. Activation of caspase-3-dependent and -independent pathways during 7-ketocholesterol- and 7beta-hydroxycholesterol-induced cell death: a morphological and biochemical study. J Biochem Mol Toxicol. 2005;19(5):311-26.

Figure legends

Fig. 1: Effect of 7β-OHC, dimethyl fumarate and monomethyl fumarate on cell growth and cell adhesion. 158N cells were cultured for 24 h with or without 7β-hydroxycholesterol (7β-OHC, 50 µM) in the presence or absence of DMF (25 µM), MMF (25 µM) or α-tocopherol (400 µM). The effects on cell growth and cell adhesion were determined by phase contrast microscopy (**A**) and crystal violet staining (**B**). Data shown are mean ± SD of three independent experiments performed in triplicate. A two way ANOVA followed by a Student's t-test was realized. Significance of the differences between 7β-OHC-treated cells and its vehicle (Ethanol (EtOH) 0.6%); # $P \leq 0.05$. Significance of the differences between 7β-OHC-treated cells, (7β-OHC + DMF), (7β-OHC + MMF) or (7β-OHC + α–tocopherol)-treated cells; * $P \leq 0.05$. No significant differences were observed between control (untreated cells), vehicle (EtOH 0.6%), and vehicle (DMSO 0.05%).

Fig. 2: Effect of 7β-OHC, dimethyl fumarate and monomethyl fumarate on cell viability and plasma membrane integrity. 158N cells were cultured for 24 h with or without 7β-hydroxycholesterol (7β-OHC, 50 µM) in the presence or absence of DMF (25 µM), MMF (25 µM) or α-tocopherol (400 µM). The effect of 7β-OHC (50 µM) with or without DMF (25 µM), MMF (25 µM) or α-tocopherol (400 µM) was determined on cell viability and plasma membrane integrity with complementary criteria: plasma membrane integrity was measured with the FDA assay (**A**), plasma membrane permeability was measured after staining with propidium iodide (PI) (% of PI positive cells) (**B**), the impact on cell viability was evaluated by the counting of living cells after staining with trypan blue (dead cells are blue whereas living cells are not) (**C**) as well as by the measurement LDH activity in the culture medium (**D**). Data shown are mean ± SD of three independent experiments performed in triplicate. A two way ANOVA followed by a Student's t-test was realized. Significance of the differences between 7β-OHC-treated cells and its vehicle (Ethanol (EtOH) 0.6%); # $P \leq 0.05$. Significance of the differences between 7β-OHC-treated cells and (7β-OHC + DMF)-, (7β-OHC + MMF)- or (7β-OHC + α–tocopherol)–treated cells; * $P \leq 0.05$. No significant differences were observed between control (untreated cells), vehicle (EtOH 0.6%), and vehicle (DMSO 0.05%).

Fig. 3: Effect of dimethyl fumarate and monomethyl fumarate on 7β-hydroxycholesterol-induced reactive oxygen species (ROS) overproduction. 158N cells were cultured for 24 h with or without 7β-hydroxycholesterol (7β-OHC; 50 µM) in the presence or absence of DMF (25 µM), MMF (25 µM), or α-tocopherol (400 µM). ROS overproduction was measured by flow cytometry; ROS

overproduction, including superoxide anion ($O_2^{\bullet -}$), was evaluated with DHE (% DHE positive cells) (**A**), and with DHR123, which takes into account hydrogen peroxide (H_2O_2) overproduction (% DHR 123 positive cells) (**B**). Data shown are mean ± SD of three independent experiments performed in triplicate. A two way ANOVA followed by a Student's t-test was realized. Significance of the difference between vehicle (ethanol (EtOH) 0.6%) and 7β-OHC-treated cells; # p≤0.05 or less. Significance of the differences between 7β-OHC-treated cells and (7β-OHC + DMF)-, (7β-OHC + MMF)- or (7β-OHC + α–tocopherol)-treated cells;* P≤0.05. No significant differences were observed between control (untreated cells), vehicle (EtOH 0.6%), and vehicle (DMSO 0.05%).

Fig. 4: Effect of dimethyl fumarate and monomethyl fumarate on 7β-hydroxycholesterol-induced oxidative stress. 158N cells were cultured for 24 h with or without 7β-hydroxycholesterol (7β-OHC, 50 µM) in the presence or absence of DMF (25 µM), MMF (25 µM) or α-tocopherol (400 µM). The effects on antioxidant enzyme activities were determined by colorimetric assays with the measurement of glutathione peroxidase (GPx) activity (**A**) superoxide dismutase (SOD) activity (**B**) and catalase (CAT) activity (**C**) as well as by the measurement of thiol-SH group (**D**). Data shown are mean ± SD of three independent experiments conducted in triplicate. A two way ANOVA followed by a Student's t-test was realized. Significance of the differences between 7β-OHC-treated cells and its vehicle (Ethanol (EtOH) 0.6%); # P≤0.05 or less. Significance of the differences between 7β-OHC-treated cells, (7β-OHC + DMF), (7β-OHC + MMF) or (7β-OHC + α-toco)-treated cells; * P≤0.05 or less. No significant differences were observed between control (untreated cells), vehicle (EtOH 0.6%), and vehicle (DMSO 0.05%).

Fig. 5: Effect of dimethyl fumarate and monomethyl fumarate on 7β-hydroxycholesterol-induced lipid peroxidation and carbonylated protein formation. 158N cells were cultured for 24 h with or without 7β-hydroxycholesterol (7β-OHC, 50 µM) in the presence or absence of DMF (25 µM), MMF (25 µM) or α-tocopherol (400 µM). The effects on lipid peroxidation product formation were evaluated by the measurement of CDs (**A**), and MDA (**B**) levels. The impact on protein oxidation was evaluated by the measurement of carbonylated protein (CPs) levels (**C**). Data shown are mean ± SD of three independent experiments performed in triplicate. A two way ANOVA followed by a Student's t-test was realized. Significance of the differences between 7β-OHC-treated cells and its vehicle (Ethanol (EtOH) 0.6%); # P≤0.05 or less. Significance of the differences between 7β-OHC-treated cells, (7β-OHC + DMF)-, (7β-OHC + MMF) or (7β-OHC + α-toco)-treated cells; * P≤0.05 or less. No significant differences were observed between control (untreated cells), vehicle (EtOH 0.6%), and vehicle (DMSO 0.05%).

Fig. 6: Evaluation of the effect of dimethyl fumarate and monomethyl fumarate on 7β-hydroxycholesterol-induced mitochondrial damage. 158N cells were cultured for 24 h with or without 7β-hydroxycholesterol (7β-OHC, 50 µM) in the presence or absence of DMF (25 µM), MMF (25 µM) or α-tocopherol (400 µM). Under these conditions, the effects succinate deshydrogenase activity were evaluated with the MTT test (**A**). The transmembrane mitochondrial potential (ΔΨm) was measured by flow cytometry after staining with $DiOC_6(3)$ (**B**). The mitochondrial mass was determined by flow cytometry after staining with MitoTracker Red (**C**). Cardiolipin levels were determined by GC-MS (**D**) and mitochondrial superoxide anion ($O_2^{\bullet -}$) production was evaluated by flow cytometry after staining with MitoSOX (**E**). Data shown are mean ± SD of three independent experiments performed in triplicate. A two way ANOVA followed by a Student's t-test was realized. Significance of the differences between 7β-OHC-treated cells and its vehicle (Ethanol (EtOH) 0.6%); # $P \leq 0.05$ or less. Significance of the differences between 7β-OHC-treated cells, (7β-OHC + DMF), (7β-OHC + MMF)- or (7β-OHC + α-toco)-treated cells; * $P \leq 0.05$ or less. No significant differences were observed between control (untreated cells), vehicle (EtOH 0.6%), and vehicle (DMSO 0.05%).

Fig. 7: Ultrastructural characterization by transmission electron microscopy of mitochondria and peroxisomes on 158N murine oligodendrocytes incubated with or without 7β-hydroxycholesterol in the presence or absence of dimethyl fumarate (DMF). 158N cells were cultured for 24 h with or without 7β-hydroxycholesterol (7β-OHC, 50 µM) in the presence or absence of DMF (25 µM). Ultrastructural aspects of mitochondria and peroxisomes in untreated (control) (**A**), DMF (**B**), 7β-OHC (**C**), and (7β-OHC + DMF) (**D**)-treated 158N cells. In the presence of 7β-OHC, several peroxisomes and mitochondria smaller than in the control were observed (**C**); these differences were no longer observed when 7β-OHC was associated with DMF (**D**). One experiment was performed.

Fig. 8: Phospholipid (sphingomyelin, phospatidylcholine) content in 158N cells exposed to 7β-hydroxycholesterol with or without dimethyl fumarate or monomethyl fumarate. 158N cells were cultured for 24 h with or without 7β-hydroxycholesterol (7β-OHC, 50 µM) in the presence or absence of DMF (25 µM), MMF (25 µM) or α-tocopherol (400 µM). Under these conditions, the quantity of sphingomyelin (SM) and phospatidylcholine (PC) per 10^6 cells was determined by GC/MS. Data shown are mean ± SD of three independent experiments performed in triplicate. A two way ANOVA followed by a Student's t-test was realized. Significance of the differences between 7β-OHC-treated cells and its vehicle (Ethanol (EtOH) 0.6%); # $P \leq 0.05$ or less. Significance of the differences between

7β-OHC-treated cells, (7β-OHC + DMF)-, (7β-OHC + MMF)- or (7β-OHC + α-toco)-treated cells; * P≤0.05 or less. No significant differences were observed between control (untreated cells), vehicle (EtOH 0.6%), and vehicle (DMSO 0.05%).

Fig. 9: Effect of dimethyl fumarate and monomethyl fumarate on 7β-hydroxycholesterol-induced morphological nuclear changes characteristic of apoptosis and lysosomal modifications evocating autophagy. 158N cells were cultured for 24 h with or without 7β-hydroxycholesterol (7β-OHC, 50 µM) in the presence or absence of DMF (25 µM), MMF (25 µM) or α-tocopherol (400 µM). Under these conditions, the quantification of the percentage of apoptotic cells was evaluated by nuclear morphologic criteria after staining with Giemsa and Hoechst 33342; apoptotic cells are characterized by condensed and/or fragmented nuclei whereas normal cells have round and regular nuclei (**A**). The impact of 7β-OHC (50 µM) with or without DMF (25 µM), MMF (25 µM) or α-tocopherol (400 µM) on the lysosome, which is involved in the autophagic process, was determined by flow cytometry after staining with acridine orange (AO); under these conditions, the percentage of AO positive cells was quantified (**B**). Data shown are mean ± SD of three independent experiments performed in triplicate. A two way ANOVA followed by a Student's t-test was realized. Significance of the differences between 7β-OHC-treated cells and its vehicle (Ethanol (EtOH) 0.6%); # P≤0.05 or less. Significance of the differences between 7β-OHC-treated cells, (7β-OHC + DMF)-, (7β-OHC + MMF)- or (7β-OHC + α-toco)-treated cells; * P≤0.05 or less. No significant differences were observed between control (untreated cells), vehicle (Ethanol 0.6%), and vehicle (DMSO 0.05%).

Fig. 10: Western blotting analysis of the effects dimethyl fumarate and monomethyl fumarate on 7β-hydroxycholesterol-induced apoptosis and autophagy on 158N murine oligodendrocytes. 158N cells were cultured for 24 h with or without 7β-hydroxycholesterol (7β-OHC, 50 µM) in the presence or absence of DMF (25 µM), MMF (25 µM) or α-tocopherol (400 µM). Apoptosis and autophagy were characterized by Western blotting with appropriate antibodies raised against uncleaved and cleaved caspase-3 and LC3-I / LC3-II, respectively. Autophagy is characterized by an enhanced (LC3-II / LC3-I) ratio. Data shown are characteristic of at least three independent experiments. A two way ANOVA followed by a Student's t-test was realized. Significance of the differences between 7β-OHC-treated cells and its vehicle (Ethanol (EtOH, 0.6%); # P≤0.05 or less. Significance of the differences between 7β-OHC-treated cells, (7β-OHC + DMF)-, (7β-OHC + MMF)- or (7β-OHC + α-toco)-treated cells; * P≤0.05 or less. No significant differences were observed between control (untreated cells), vehicle (EtOH 0.6%), and vehicle (DMSO 0.05%).

Fig. 11: Evaluation of protein kinase A (PKA), phospholipase C (PLC)/protein kinase C (PKC) and MEK / ERK signaling pathways in 7β-OHC-induced cell death on 158N cells. Murine oligodendrocyte 158N cells previously cultured for 24 h were further cultured for 24 h with or without 7β-OHC (50 µM) in the presence or absence of different inhibitors, H89, U0126, U73122 and chelerythrine, introduced 30 min before the addition of 7β-OHC. Data shown are mean ± SD of two independent experiments performed in triplicate. A two way ANOVA followed by a Student's t-test was realized. No significant difference was observed between control (untreated cells), vehicle (ethanol (EtOH): 0.6%)-treated cells and inhibitors (H89, U0126, U73122 or chelerythrine)-treated cells. Significance of the differences between 7β-OHC-treated cell and vehicle (EtOH 0.6%); # $P \leq 0.05$ or less. Significant of the differences between 7β-OHC-treated cells and (7β-OHC + (H89, U0126, U73122, or chelerythrine))-treated cells: * $P \leq 0.05$.

Fig. 12: Effects of dimethyl fumarate and mono methyl fumarate on the recovery of 7β-hydroxycholesterol-induced cell death. In these experiments, after 24 h of culture, 158N cells were incubated with 7β-OHC (50 µM) for 6 h before the addition of DMF (25 µM), MMF (25 µM), or α-tocopherol (400 µM). The cells were subsequently incubated with 7β-OHC (50 µM) associated with DMF, MMF or α-tocopherol for an 18 h additional period of time. **A**: total number of living cells evaluated after staining with trypan blue; **B**: percentage of cells with apoptotic nuclei determined after staining with Hoechst 33342. Data shown are mean ± standard deviation (SD) of three independent experiments performed in triplicate. A two way ANOVA followed by a Student's t-test was realized. Significant differences between 7β-OHC-treated cells and the vehicle (ethanol (EtOH, 0.6%): # $P \leq 0.05$. Significant differences between 7β-OHC-treated cells and (7β-OHC + DMF)-, (7β-OHC + MMF)- or (7β-OHC + α–tocopherol)–treated cells; * $P \leq 0.05$. No significant differences were observed between control (untreated cells), vehicle (EtOH 0.6%), and vehicle (DMSO 0.05%).

Supplementary Fig. 1: Estimation of the 50% inhibiting concentration of 7β-hydroxycholesterol on the viability of murine oligodendrocytes 158N. 158N cells previously cultured for 24 h were further incubated for 24 h with or without 7β-hydroxycholesterol (7β-OHC: 1, 6.25, 12.5, 25, 50, 100, 200 µM). In those conditions, the cytotoxicity was determined with the MTT test. Vehicle: EtOH 0.6%. Data shown are mean ± SD (Two experiments realized in triplicate). A one way ANOVA followed by a Student's t-test was realized. Significance of the differences between 7β-OHC-treated cells and vehicle (Ethanol (EtOH) 0.6%)-treated cells; # $P \leq 0.05$ or less. No difference was observed between control (untreated cells) and vehicle (EtOH 0.6%)-treated cells.

Supplementary Fig. 2: Evaluation of the optimal concentration of DMF and MMF preventing 7β-hydroxycholesterol-induced cytotoxicity on murine oligodendrocytes 158N. 158N cells previously cultured for 24 h were further incubated for 24 h with or without 7β-hydroxycholesterol (7β-OHC, 50 µM) in the presence or absence of DMF or MMF (1, 12.5, 25, 50 and 100 µM). In these conditions, the cytotoxicity was determined with the MTT test. Vehicles: ethanol (EtOH, 0.6%) or DMSO (0.002, 0.025, 0.05, 0.1, 0.2%). Data shown are mean ± SD of three independent experiments realized in triplicate. A two way ANOVA followed by a Student's t-test was realized. No significant differences were observed between control (untreated cells), and vehicle (EtOH or DMSO). Significant differences between 7β-OHC-treated cells and the vehicle (EtOH: 0.6%): # $P \leq 0.05$. Significant differences between 7β-OHC-treated cells and (7β-OHC + DMF)- or (7β-OHC + MMF)-treated cells; * $P \leq 0.05$.

Supplementary Fig. 3: Determination of the Ct values of the gene HSD11B1 encoding for the enzyme 11β-HSD1 in murine oligodendrocytes 158N and murine microglial BV-2 cells. The amplification plots and the melt curves of HSD11B1 are shown for 158N and BV-2 cells. The Ct values of HSD11B1 and of the reference gene 36B4 are also shown. Data shown are representative of 3 independent experiments realized in triplicate.

Supplementary Fig. 4: Determination of the Ct values of the gene HSD11B1 encoding for the enzyme 11β-HSD1 in murine oligodendrocytes 158N and murine microglial BV-2 cells. The amplification plots and the melt curves of HSD11B2 are shown for 158N and BV-2 cells. The Ct values of HSD11B2 and of the reference gene 36B4 are also shown as well as the expression of HSD11B2 in 158N cells (158N cells previously cultured for 24 h were further incubated for 24 h with or without 7β-OHC (50 µM) in the presence or absence of DMF or MMF (25 µM); the quantitative induction of HSD11B2 was determined as fold induction of the control; a two way ANOVA followed by a Student's t-test was realized: no significant difference was observed). Data shown are representative of 1 experiment realized in triplicate.

Supplementary Fig.5 : Determination of the time of treatment with dimethyl fumarate and monomethyl fumarate for recovery of 7β-hydroxycholesterol-induced cell death. The effect of DMF and MMF (25 µM) or α-tocopherol (400 µM) on 7β-OHC (50 µM)-induced cell death was determined with the FDA test when biotin or α-tocopherol were added after 7β-OHC (6 and 10 h). The most efficient time to prevent 7β-OHC-induced cell death when α-tocopherol and biotin were introduced in the culture medium after 7β-OHC was 6 h. Data shown are mean ± SD (Two

independent experiments realized in triplicate). A two way ANOVA followed by a Student's t-test was realized. No significant differences were observed between control (untreated cells), and vehicle (ethanol (EtOH) 0.6% or DMSO 0.05%). Significant differences between treated cells and the vehicle (EtOH: 0.6%): # P≤0.05. Significant differences between 7β-OHC-treated cells and (7β-OHC + DMF), (7β-OHC + MMF) or (7β-OHC + α–tocopherol)–treated cells; * P≤0.05.

Supplementary Fig. 6: Analysis of myelin protein expression (PLP, MBP) in 158N cells. Murine oligodendrocytic 158N cells were cultured for 24 h with or without 7β-hydroxycholesterol (7β-OHC, 50 µM) in the presence or absence of DMF (25 µM), MMF (25 µM), or α-tocopherol (400 µM). The major myelin proteins PLP and MBP as well as actin (used as internal reference) were characterized by Western blotting with appropriate antibodies. Vehicles: ethanol (ethanol (EtOH) 0.6%; DMSO 0.05%. Data are mean ± SD of three independent experiments. A two way ANOVA followed by a Student's t-test was realized. Significance of the differences between 7β-OHC-treated cells and its vehicle (EtOH 0.6%); # P≤0.05 or less. Significance of the differences between 7β-OHC-treated cells, (7β-OHC + DMF)-, (7β-OHC + MMF)- or (7β-OHC + α-toco)-treated cells; * P≤0.05 or less.

Supplementary Fig. 7: Schematic signalling pathways associated with 7β-hydroxycholesterol-induced oxiapoptophagy. The schematic signalling patways presented summarizes the data obtained from different cell types [**3, 8, 16, 18, 19, 84**]. In the different cell types studied, 7β-OHC is a strong inducer of reactive oxygen species (ROS) overproduction. In 158N cells, 7β-OHC also favors the disturbance of Redox homeostasis by increasing the formation of lipid peroxidation products (malondialdehyde (MDA), conjugated dienes (CDs)) and of carbonylated proteins (CPs) which can further contribute to cell death. Important impact on the mitochondria was also observed whatever the cells are considered. In human monocytic THP-1 and U937 cells, a down-regulation of Bcl-2 expression was also detected as well as an activation of the pro-apoptotic proteins (Bid, Bax), associated with a release of cytochrome c and an activation of caspase-9, caspase-8, caspase-3 and caspase-7. In U937 cells, 7β-OHC also induced an increase in cytosolic Ca^{2+} concentration, associated with a decrease of Akt activation and a mitochondrial release of various proteins such as cytochrome c, apoptosis-inducing factor (AIF), and endonuclease-G (Endo-G), associated with caspase-3, -7, -8, and -9 activation, Bid cleavage and poly(ADP-ribose)polymerase (PARP) degradation. In C6 glioblastoma cells, 7β-OHC induces apoptosis through the decrease of ERK signalling, the transient PI3K / Akt activation, the loss of GSK3β activation and the activation of p38. The data obtained in the present study on 158N cells support that p38 activation could be triggered by PKC. On U937 cells as well as

on human retinal pigment epithelial cells (ARPE-19), large myelin figures (evocating reticulophagy) were observed. On ARPE-19 cells, a link between lysosome and cell death was also established. In 158N cells, the complex mode of cell death induced by 7β-OHC (oxiapoptophagy) is characterized by a dephosphorylation of PKB / Akt, an activation of GSK3, and by a reduced expression of Bcl-2; altogether these events contribute to mitochondrial depolarization leading to caspase-3 activation, PARP degradation and internucleosomal DNA fragmentation. Moreover, 7β-OHC promotes the conversion of microtubule-associated protein light chain 3 (LC3-I) to LC3-II which is a criteria of autophagy. Altogether, these data establish that 7β-OHC is a potent inducer of oxiapoptophagy through the concomittent activation of several signalling pathways involved in oxidative stress, apoptosis and autophagy.

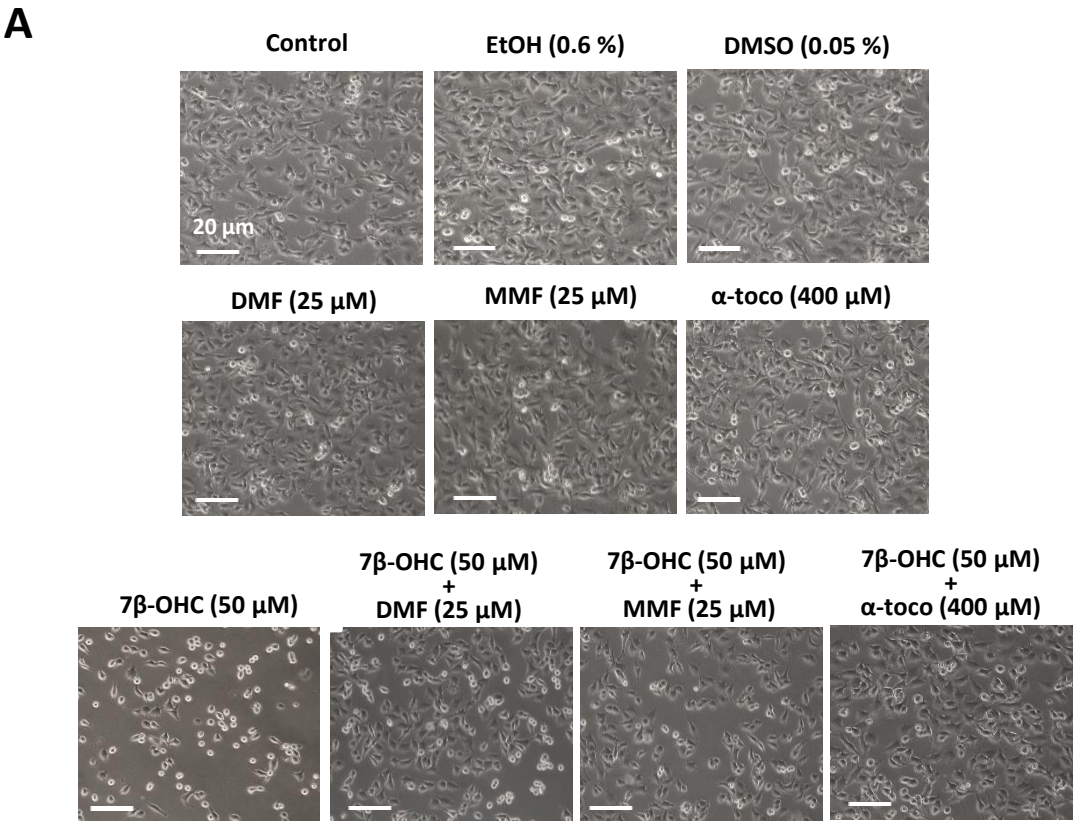

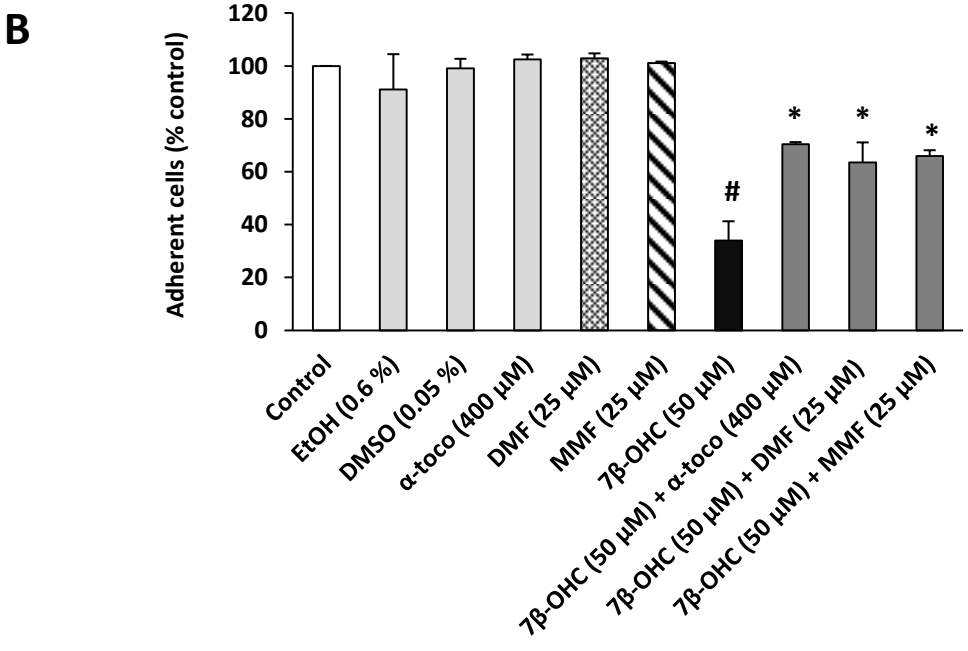

Fig. 1; Sghaier R et al

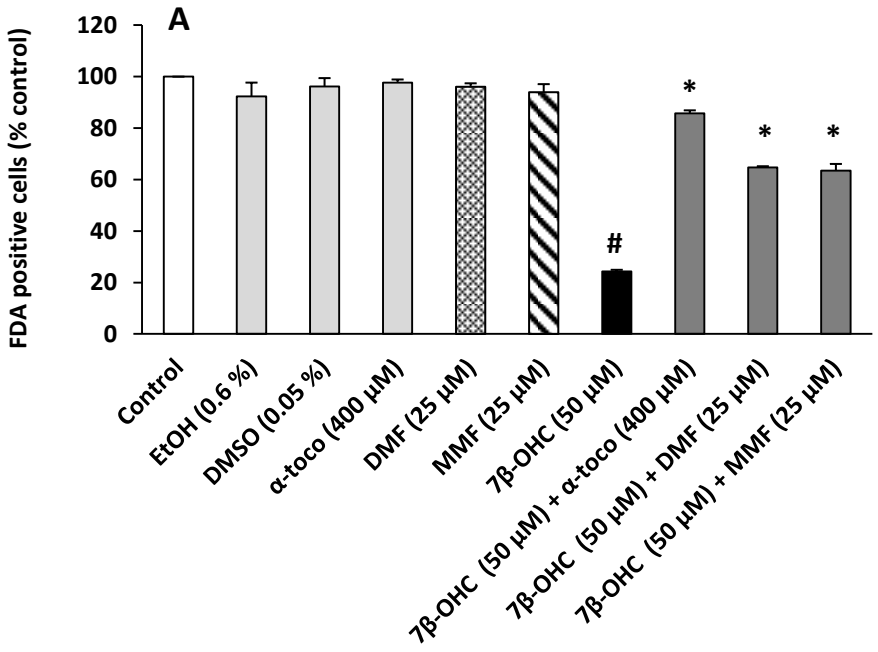

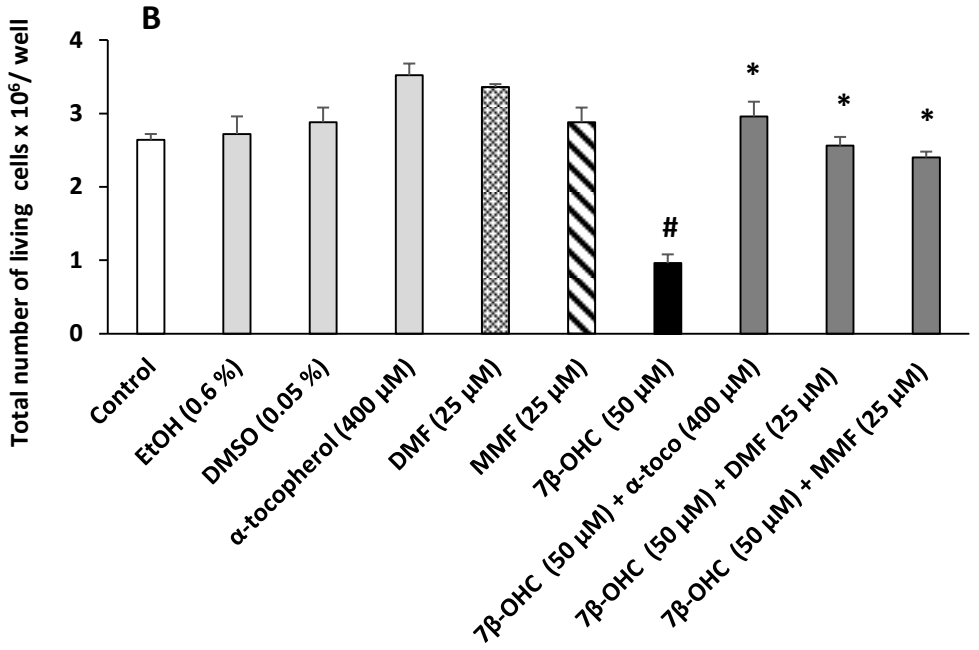

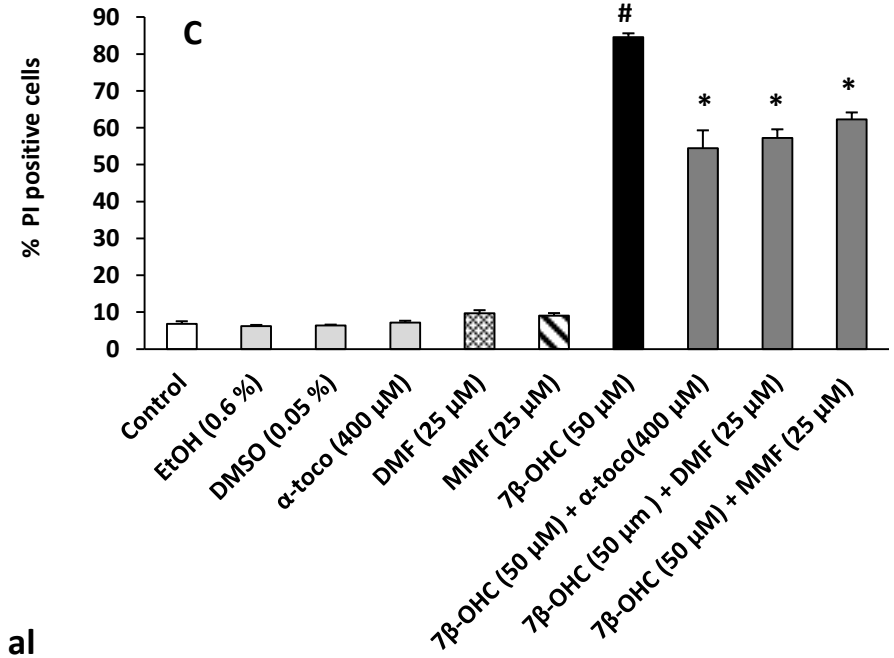

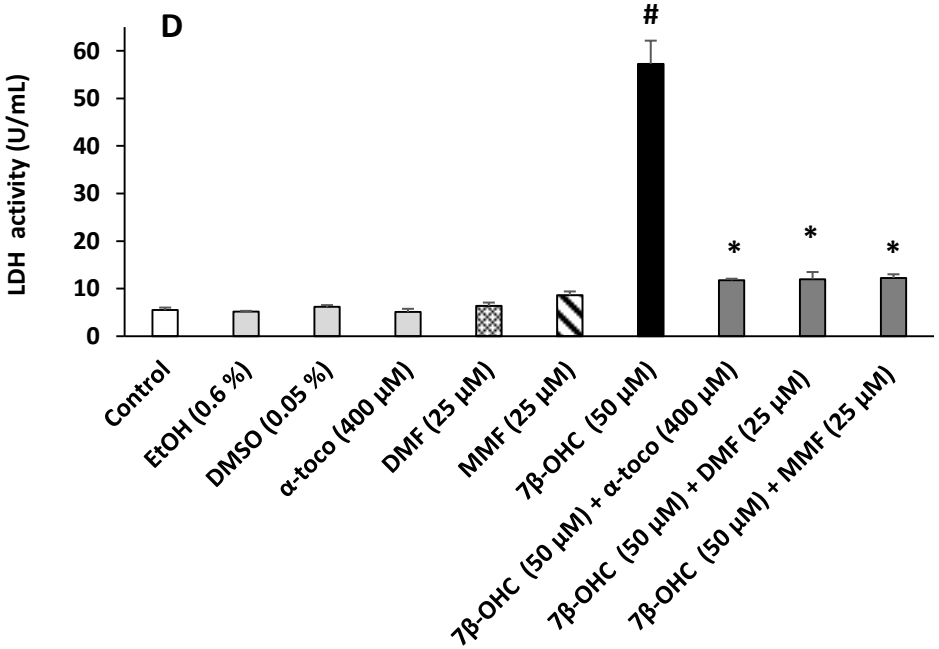

Fig. 2; Sghaier R et al

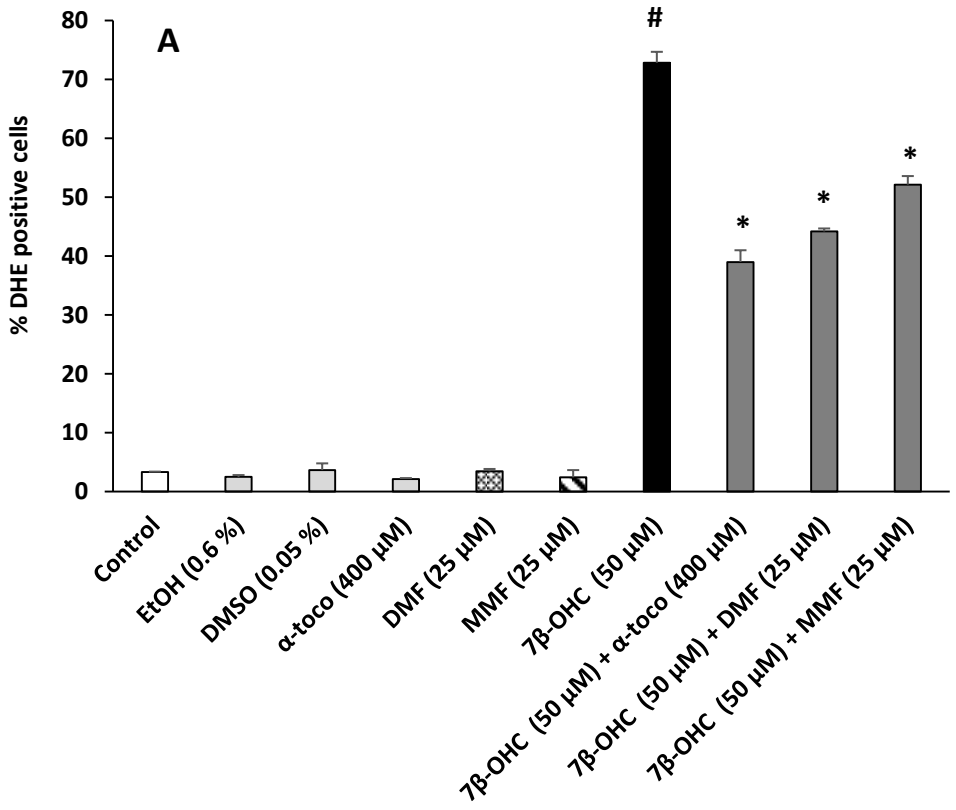

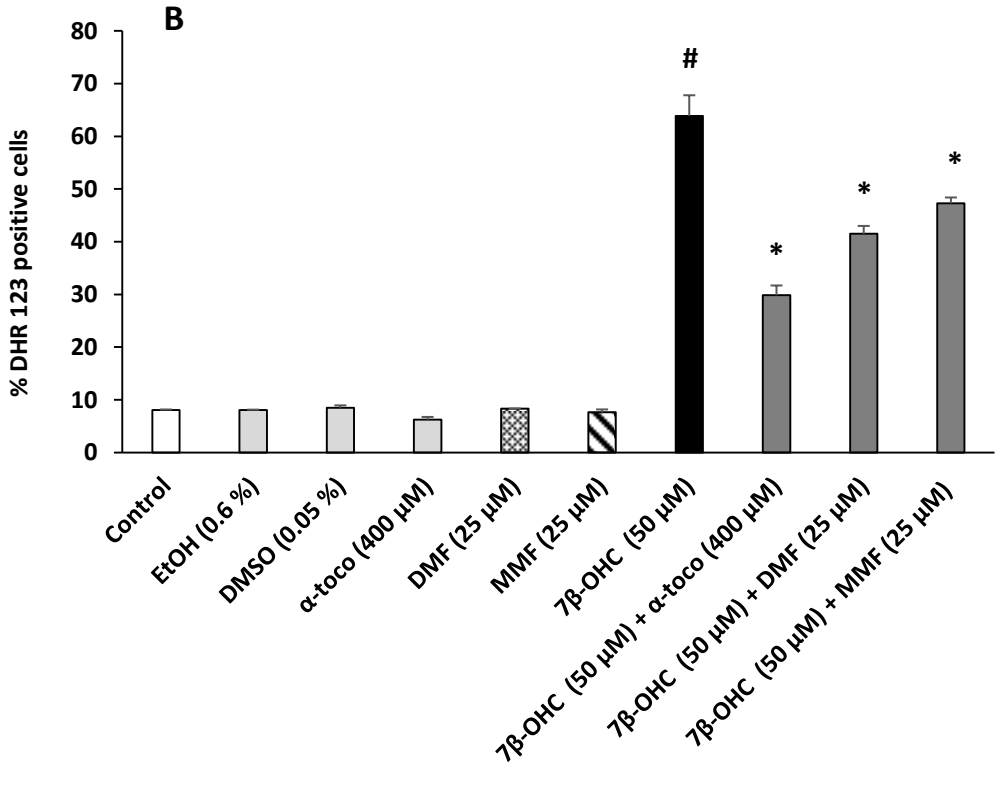

Fig. 3; Sghaier R et al

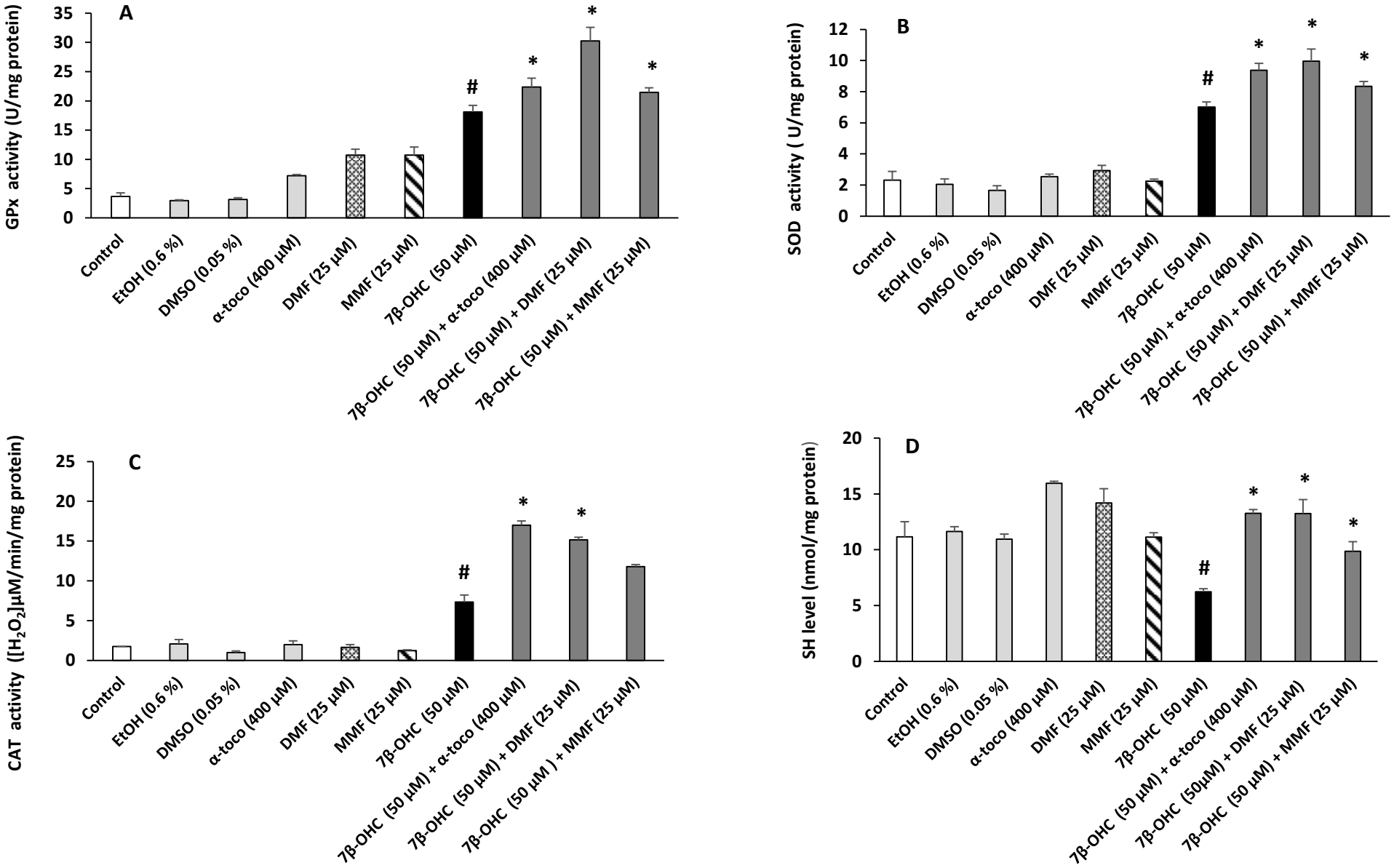

Fig. 4; Sghaier R et al

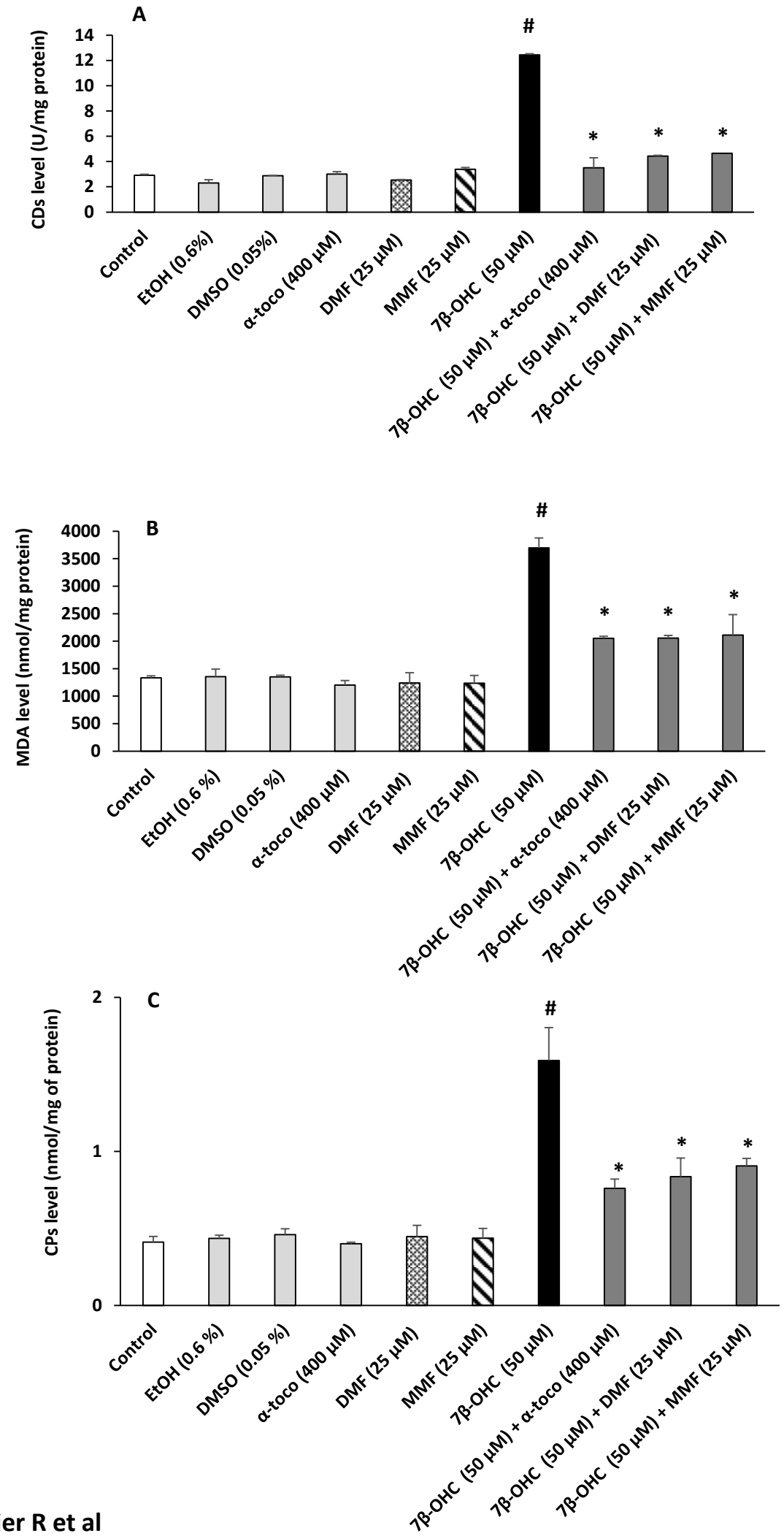

Fig. 5; Sghaier R et al

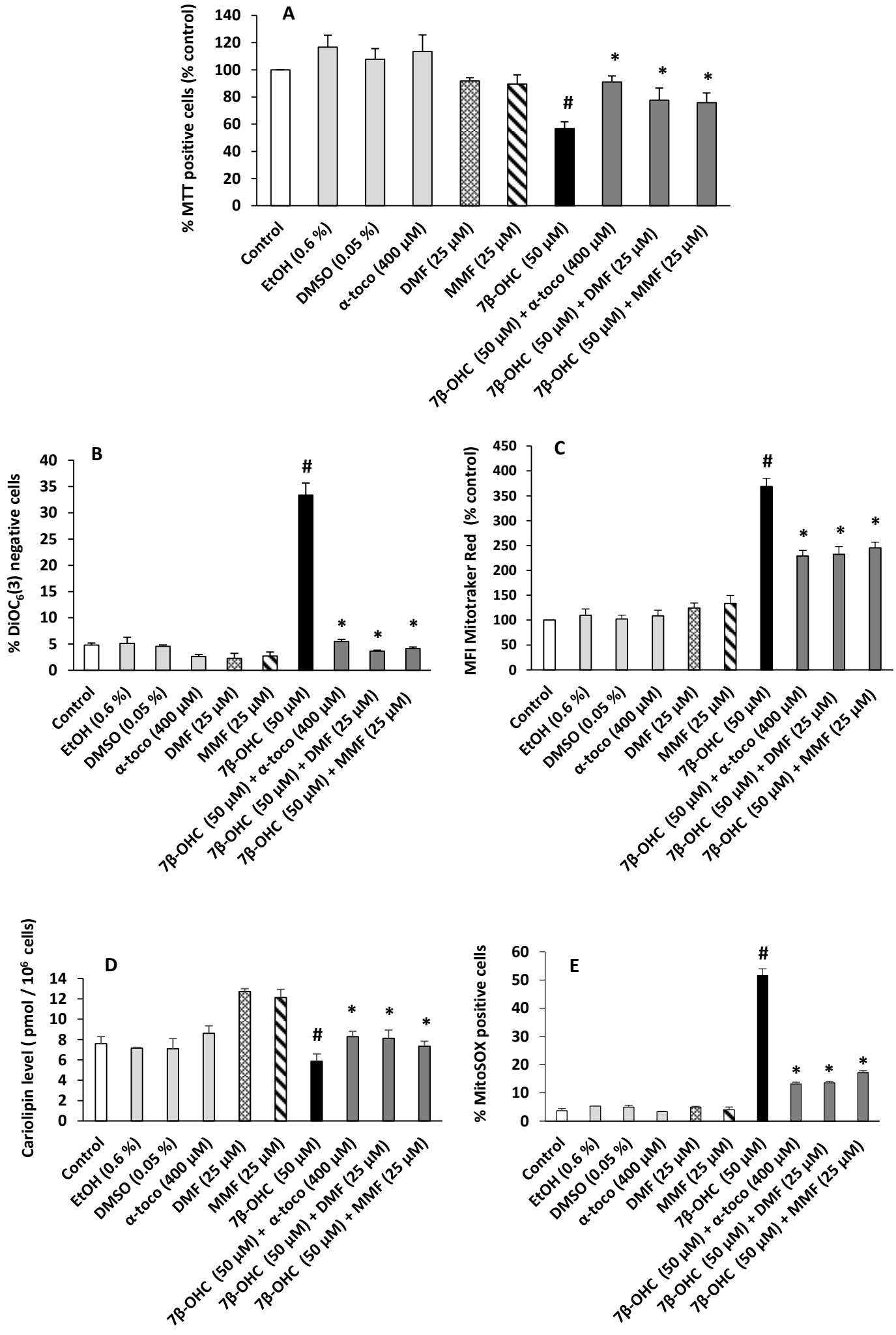

Fig. 6; Sghaier R et al

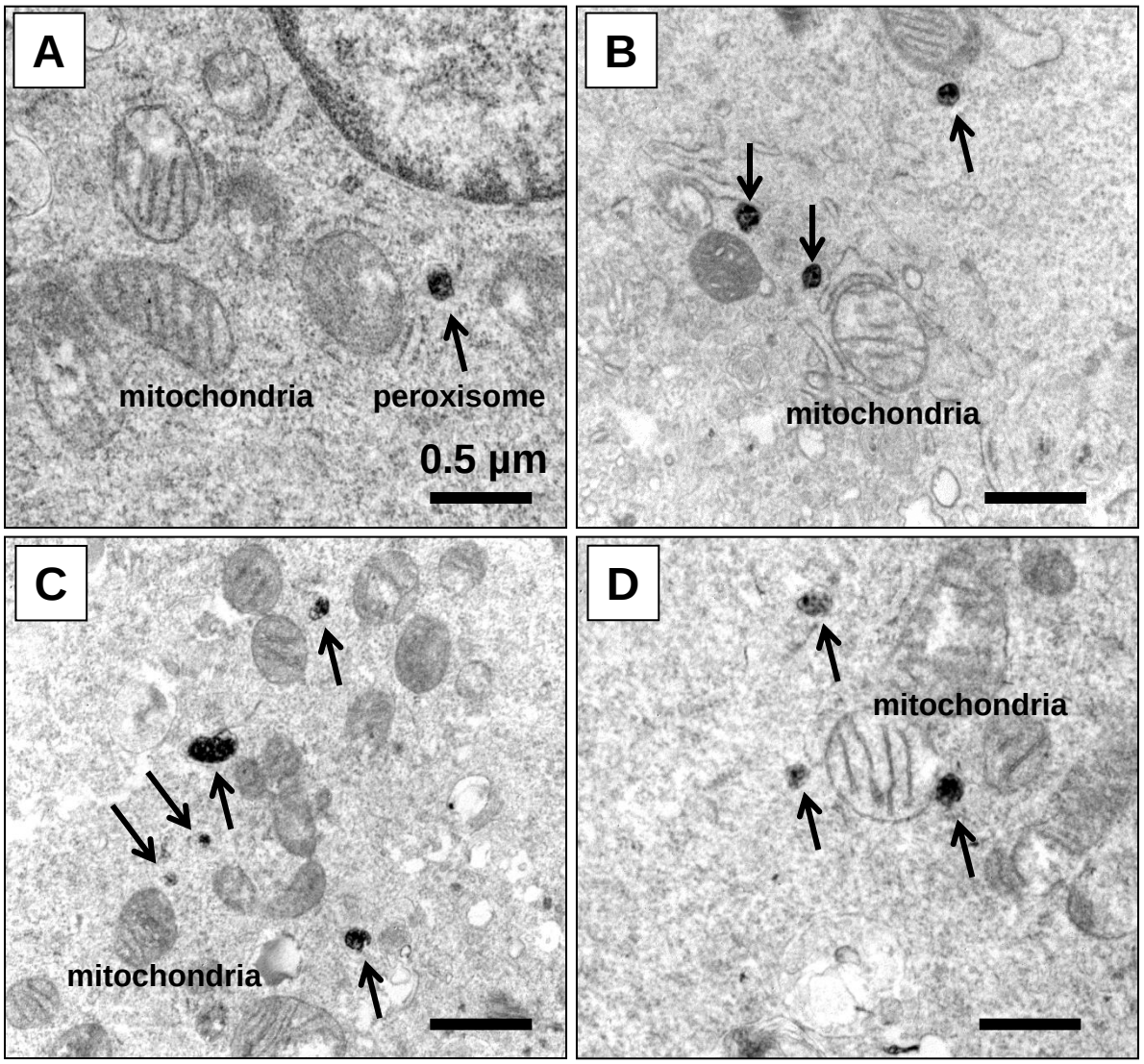

Fig. 7; Sghaier R et al

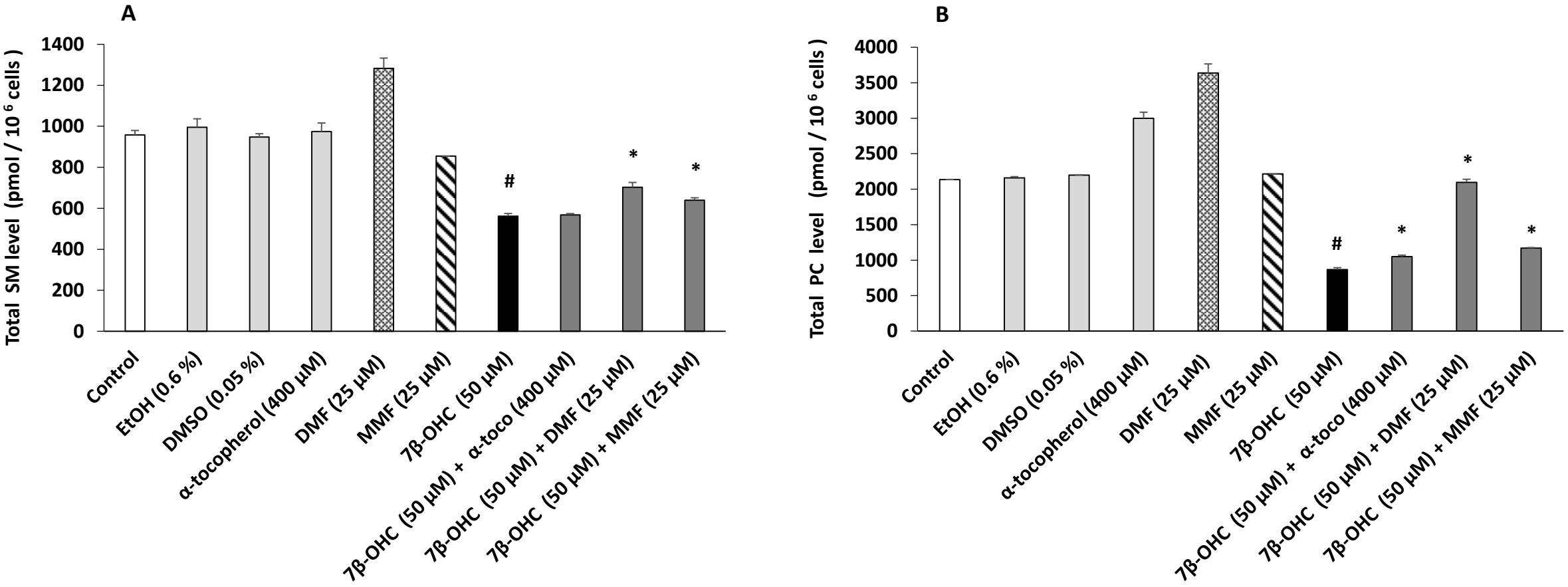

Fig. 8; Sghaier R et al

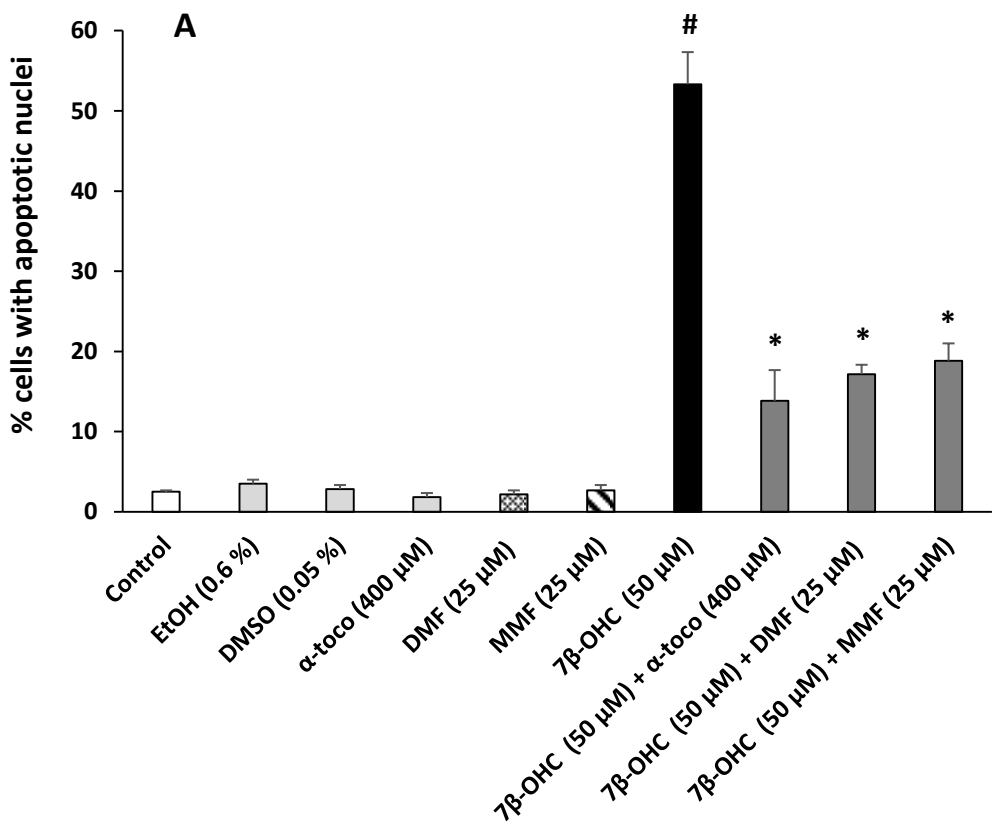

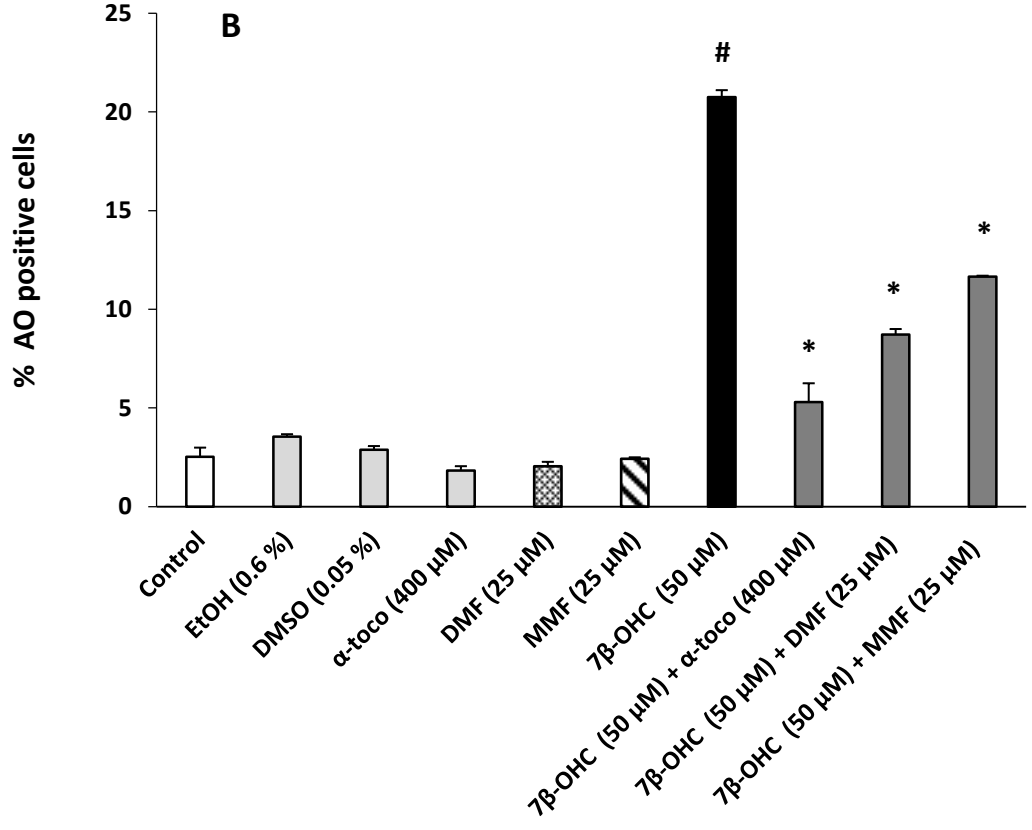

Fig. 9; Sghaier R et al

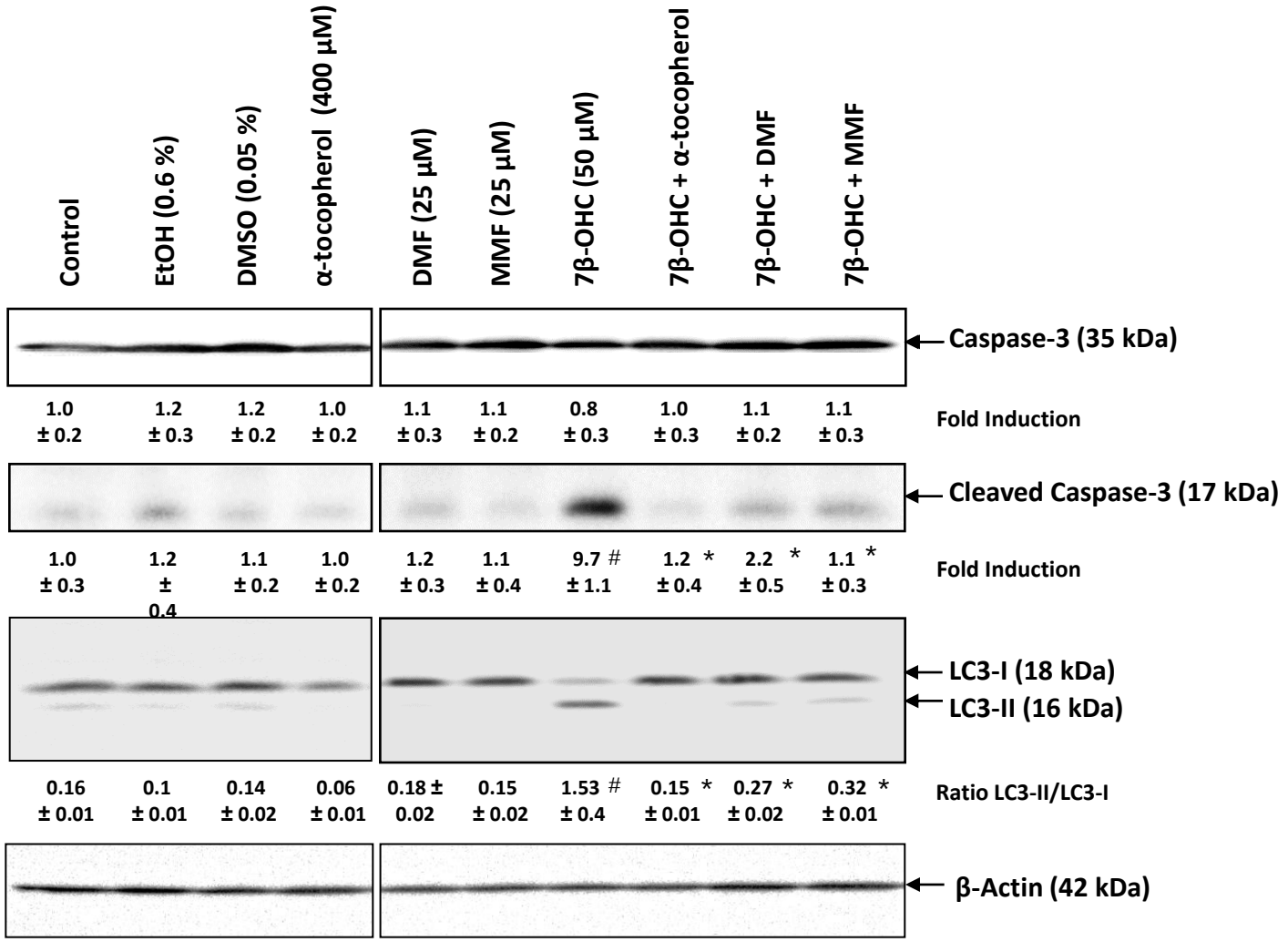

Fig. 10; Sghaier R et al

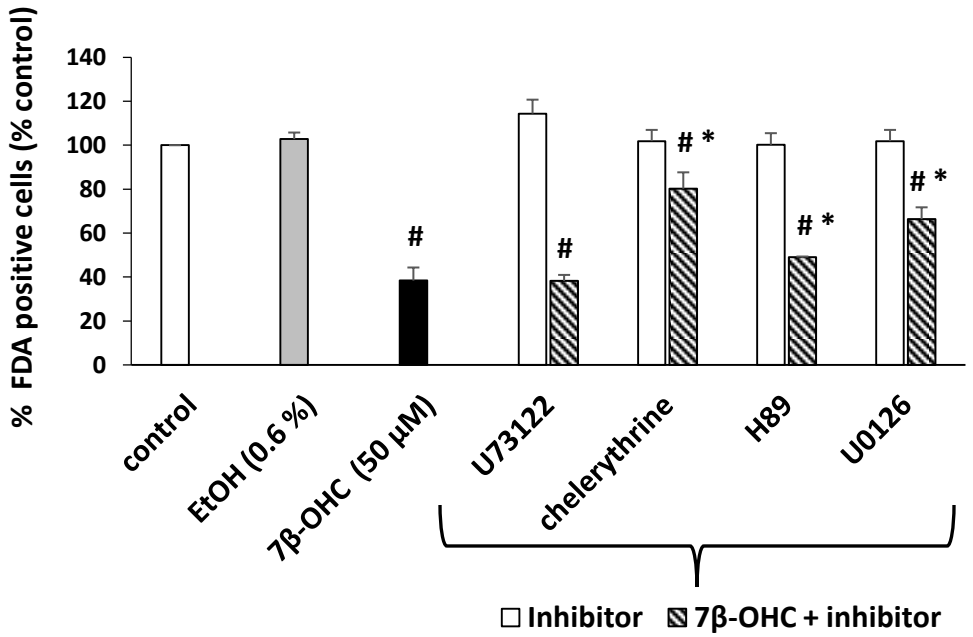

Fig. 11; Sghaier R et al

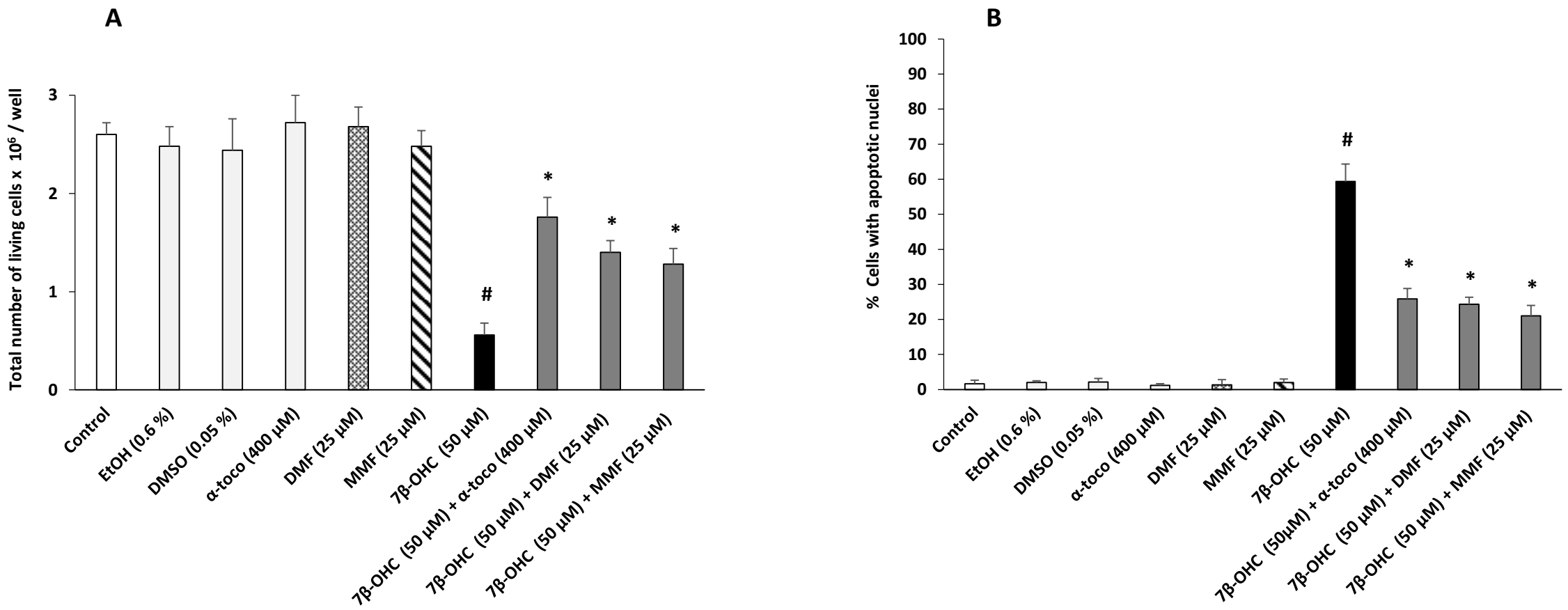

Fig. 12; Sghaier R et al

Table 1: Profile of organic acids in 158N cells exposed to 7β-hydroxycholesterol with or without dimethyl fumarate (DMF) or monomethyl fumarate (MMF)

	Lactic acid	Pyruvic acid	Succinic acid	Fumaric acid	Malic acid	Citric acid
Control	126.98 ± 7.99	15.27 ± 0.36	7.55 ± 0.11	1.33 ± 0.04	3.69 ± 0.10	4.79 ± 0.20
EtOH (0.6%)	122.64 ± 3.53	14.13 ± 0.50	6.82 ± 0.05	1.22 ± 0.06	2.54 ± 0.08	3.84 ± 0.11
DMSO (0.05%)	125.90 ± 12.62	13.43 ± 0.78	6.88 ± 0.11	1.30 ± 0.03	2.36 ± 0.03	4.60 ± 0.06
DMF (25 µM)	97.30 ± 1.51	16.43 ± 1.48	6.97 ± 0.73	2.66 ± 0.21	3.88 ± 0.22	5.89 ± 0.16
MMF (25 µM)	104.84 ± 3.45	15.46 ± 0.01	7.18 ± 0.11	2.72 ± 0.05	4.93 ± 0.17	6.34 ± 0.04
7β-OHC (50 µM)	220.59 ± 2.50 #	8.11 ± 0.06 #	5.46 ± 0.01 #	0.93 ± 0.02 #	1.75 ± 0.08 #	2.80 ± 0.25 #
7β-OHC (50 µM) + DMF (25 µM)	147.63 ± 6.46*	15.64 ± 0.87*	7.41 ± 0.58*	1.35 ±0.16 *	4.67 ± 0.11*	3.60 ± 0.05*
7β-OHC (50 µM) + MMF (25 µM)	120.84 ± 4.03*	12.55 ± 1.35*	11.48 ± 0.45*	1.78 ± 0.00*	3.59 ± 0.08*	4.07 ± 0.08*

Concentrations are expressed as ng/million cells.
*Results are expressed as mean ± SD of three independent experiments. A two way ANOVA followed by a Student's t-test was realized. Significant difference between vehicle (EtOH 0.6%) and 7β-OHC-treated cells is indicated by #; P < 0.05; significant difference between 7β-OHC and (7β-OHC + DMF) or (7β-OHC + MMF) is indicated by *; P < 0.05.*
No significant differences are observed between Control, EtOH and DMSO. 7β-hydroxycholesterol: 7β-OHC.

Table 2: Profiles of cholesterol, cholesterol precursors (lathosterol, desmosterol, lanosterol) and oxysterols (triol, 7-ketocholesterol, 7β–hydroxycholesterol) in 158N cells exposed to7β–hydroxycholesterol with or without dimethyl fumarate (DMF) or monomethyl fumarate (MMF)

	Cholesterol	Cholesterol precursors			Oxysterols		
		Lathosterol	*Desmosterol*	*Lanosterol*	*Triol*	*7KC*	*7β-OHC*
Control	2.84 ± 0.01	14.80 ± 0.15	12.93 ± 0.37	0.63 ± 0.00	0.17 ± 0.01	0.56 ± 0.02	0.62 ± 0.00
EtOH (0.6%)	2.86 ± 0.02	14.08 ± 0.02	12.08 ± 0.13	0.58 ± 0.02	0.12 ± 0.01	0.59 ± 0.00	0.66 ± 0.04
DMSO (0.05%)	2.64 ± 0.03	13.64 ± 0.36	10.01 ± 0.42	0.45 ± 0.03	0.08 ± 0.01	0.42 ± 0.06	0.56 ± 0.02
DMF (25 µM)	2.72 ± 0.11	14.93 ± 0.19	9.58 ± 0.26	0.65 ± 0.02	0.09 ± 0.02	0.51 ± 0.00	0.62 ± 0.07
MMF (25 µM)	2.83 ± 0.10	17.10 ± 0.94	10.07 ± 0.50	0.69 ± 0.03	0.05 ± 0.01	0.60 ± 0.09	2.94 ± 0.07
7β-OHC (50 µM)	2.17 ± 0.13 #	8.53 ± 0.17 #	6.46 ± 0.07 #	0.23 ± 0.01 #	1.89 ± 0.16 #	10.88 ± 0.34 #	246.70 ± 0.59 #
7β-OHC (50 µM) + DMF (25 µM)	2.56 ± 0.05 *	5.33 ± 0.14 *	6.20 ± 0.07*	0.66 ± 0.03 *	0.86 ± 0.01 *	5.72 ± 0.39 *	470.12 ± 9.95 *
7β-OHC (50 µM) + MMF (25 µM)	2.16 ± 0.12	6.72 ± 0.34 *	5.08 ± 0.21 *	0.32 ± 0.00*	0.88 ± 0.29 *	9.33 ± 0.47 *	426.67 ± 6.19 *

Concentrations are expressed as ng/million cells.

*Results are expressed as mean ± SD of three independent experiments. A two way ANOVA followed by a Student's t-test was realized. Significant difference between vehicle (EtOH 0.6%) and 7β-OHC-treated cells is indicated by #; P < 0.05; significant difference between 7β-OHC and (7β-OHC + DMF) or (7β-OHC + MMF) is indicated by *; P < 0.05. No significant differences are observed between Control, EtOH and DMSO.*

7β-hydroxycholesterol: 7β-OHC.

Table 3: Profile of saturated fatty acids in 158N cells exposed to 7β-hydroxycholesterol withor without dimethyl fumarate (DMF) or monomethyl fumarate (MMF)

	Control	EtOH (0.6%)	DMSO (0.05%)	DMF (25 µM)	MMF (25 µM)	7β-OHC (50 µM)	7β-OHC (50 µM) + DMF (25 µM)	7β-OHC (50 µM) + MMF (25 µM)
C14:0	109.48 ± 0.30	101.56 ± 0.86	79.45 ± 0.46	98.99 ± 3.83 ¥	99.55 ± 5.57 ¥	81.82 ± 0.36 #	49.48 ± 4.56 *	85.74 ± 5.30
C16:0	2360.32 ± 25.67	2300.14 ± 40.89	2247.38 ± 8.37	1934.86 ± 20.36 ¥	2320.20 ± 45.94 ¥	1727.54 ± 29.59 #	1650.60 ± 14.00 *	2553.74 ± 23.91 *
C18:0	1240.25 ± 21.80	1169.50 ± 22.09	941.92 ± 10.14	875.63 ± 22.65 ¥	1338.75 ± 7.60 ¥	722.54 ± 16.83 #	805.03 ± 6.67 *	829.81 ± 2.14 *
C20:0	29.40 ± 2.49	24.36 ± 1.17	25.19 ± 1.26	20.04 ± 0.64 ¥	19.90 ± 0.05 ¥	10.83 ± 1.14 #	8.61 ± 1.03 *	13.59 ± 0.25 *
C22:0	4.61 ± 0.54	4.49 ± 0.18	4.69 ± 0.01	4.38 ± 0.12 ¥	4.79 ± 0.53	8.19 ± 0.26 #	5.97 ± 0.06 *	6.68 ± 0.49 *
C24:0	8.32 ± 0.31	8.27 ± 0.18	7.68 ± 0.03	8.61 ± 0.36 ¥	11.10 ± 3.24 ¥	24.58 ± 0.84 #	7.52 ± 0.70 *	10.22 ± 0.58 *
C26:0	1.47 ± 0.13	1.51 ± 0.28	1.56 ± 0.04	3.78 ± 0.24 ¥	2.54 ± 0.07 ¥	11.85 ± 0.91 #	5.79 ± 0.45*	7.96 ± 0.34 *
∑SFA (C<22)	3739.44 ± 44.69	3595.56 ± 16.77	3293.94 ± 0.05	2929.52 ± 2.18 ¥	3778.41 ± 59.16 ¥	2542.72 ± 14.26 #	2513.71 ± 26.26	3482.88 ± 31.60 *
∑VLCSFA C≥22)	14.40 ± 0.98	14.27 ± 0.08	13.93 ± 0.07	16.78 ± 0.71 ¥	18.42 ± 3.85¥	44.62 ± 2.01 #	19.28 ± 1.09 *	24.87 ± 1.42 *
∑total SFA	3753.84 ± 43.70	3609.83 ± 16.69	3307.87 ± 0.02	2946.30 ± 1.47 ¥	3796.83 ± 63.00 ¥	2587.34 ± 12.25 #	2533.00 ± 27.35 *	3507.75 ± 30.18 *

Concentrations are expressed as ng/million cells.

*Results are expressed as mean ± SD of three independent experiments. A two way ANOVA followed by a Student's t-test was realized. Significant difference between vehicle (EtOH 0.6%) and 7β-OHC-treated cells is indicated by #; P < 0.05; significant difference between 7β-OHC and (7β-OHC + DMF) or (7β-OHC + MMF) is indicated by *; P < 0.05; significant difference between vehicle (DMSO 0.05%) and DMF or MMF treated cells is indicated by ¥; P < 0.05. No significant differences are observed between Control, EtOH and DMSO.*

∑ ***SFA:*** *Sum of saturated fatty acids;* ∑ ***VLCSFA:*** *Sum of very long chain saturated fatty acids; 7β-hydroxycholesterol: 7β-OHC.*

Table 4: Profile of mono-unsaturated fatty acids profile in 158N cells exposed to 7β-hydroxycholesterol with or without dimethyl fumarate (DMF) and monomethyl fumarate (MMF)

	Control	EtOH (0.6%)	DMSO (0.05%)	DMF (25 µM)	MMF (25 µM)	7β-OHC (50 µM)	7β-OHC (50 µM) + DMF (25 µM)	7β-OHC (50 µM) + MMF (25 µM)
C14:1 n-5	2.19 ± 0.00	2.10 ± 0.02	1.53 ± 0.22	2.22 ± 0.16 ¥	3.29 ± 0.16 ¥	1.61 ± 0.09 #	1.82 ± 0.05 *	1.71 ± 0.20
C16:1 n-10 or n-9	231.31 ± 6.96	230.16 ± 9.14	175.46 ± 3.55	176.83 ± 13.98	241.36 ± 6.80 ¥	207.41 ± 6.36 #	274.92 ± 6.32 *	276.70 ± 14.62 *
C16:1 n-7	454.04 ± 26.71	420.16 ± 28.80	352.91 ± 10.09	400.29 ± 4.27 ¥	553.16 ± 11.81 ¥	313.62 ± 11.98 #	373.66 ± 2.06 *	545.29 ± 4.92 *
C18:1 n-9	2239.11 ± 16.15	2035.46 ± 48.32	1812.39 ± 30.35	2053.93 ± 47.61 ¥	2487.96 ± 8.81 ¥	1970.72 ± 36.33	1746.52 ± 0.25 *	1759.29 ± 0.74 *
C18:1 n-7	502.24 ± 8.92	464.92 ± 46.02	448.74 ± 28.15	546.50 ± 18.31 ¥	718.05 ± 51.47 ¥	403.71 ± 2.75 #	452.47 ± 31.14 *	439.80 ± 1.16 *
C20:1 n-9	62.63 ± 3.25	54.37 ± 0.23	56.61 ± 2.99	91.13 ± 8.80 ¥	84.90 ± 4.67 ¥	16.82 ± 0.11 #	55.57 ± 0.17 *	55.03 ± 1.27 *
C20:1 n-7	32.03 ± 0.04	34.63 ± 0.47	35.26 ± 0.16	24.77 ± 2.21 ¥	27.13 ± 0.48 ¥	5.65 ± 1.00 #	12.83 ± 0.45 *	14.74 ± 0.40 *
C22:1 n-9	2.37 ± 0.05	2.34 ± 0.04	2.00 ± 0.06	2.96 ± 0.14 ¥	2.85 ± 0.25 ¥	2.29 ± 0.16	3.06 ± 0.20 *	2.25 ± 0.11
C24:1 n-9	12.58 ± 0.53	13.01 ± 0.01	14.61 ± 0.51	22.37 ± 0.58 ¥	24.19 ± 1.78 ¥	32.71 ± 0.96 #	23.52 ± 1.44 *	23.99 ± 2.85 *
C26:1 n-9	0.59 ± 0.03	0.62 ± 0.00	0.57 ± 0.04	1.25 ± 0.05 ¥	1.32 ± 0.05 ¥	2.27 ± 0.08 #	1.30 ± 0.02 *	1.64 ± 0.03 *
∑MUFA	3539.09 ± 47.48	3257.77 ± 17.64	2900.09 ± 13.39	3322.26 ± 78.18 ¥	4144.22 ± 55.05¥	2956.82 ± 13.18 #	2945.67 ± 20.57	3120.44 ± 22.97 *

Concentrations are expressed as ng/million cells.

*Results are expressed as mean ± SD of 3 independent experiments. A two way ANOVA followed by a Student's t-test was realized. Significant difference between vehicle (EtOH 0.6%) and 7β-OHC-treated cells is indicated by **#**; P < 0.05; significant difference between 7β-OHC and (7β-OHC + DMF) or (7β-OHC + MMF) is indicated by *; P < 0.05; significant difference between vehicle (DMSO 0.05%) and DMF or MMF treated cells is indicated by ¥; P < 0.05. No significant differences are observed between Control, EtOH and DMSO. **∑MUFA:** Sum of mono-saturated fatty acids; 7β-hydroxycholesterol: 7β-OHC.*

Sghaier R et al.

Table 5: Profile of polyunsaturated fatty acids in 158N cells exposed to 7β-hydroxycholesterol with or without dimethyl fumarate (DMF) or monomethyl fumarate (MMF)

	Control	EtOH (0.6%)	DMSO (0.05%)	DMF (25 µM)	MMF (25 µM)	7β-OHC (50 µM)	7β-OHC (50 µM) + DMF (25 µM)	7β-OHC (50 µM) + MMF (25 µM)
C18:2 n-6	32.66 ± 2.10	28.06 ± 0.94	29.72 ± 0.41	36.30 ± 1.14 ¥	36.77 ± 3.82 ¥	23.14 ± 1.48 #	26.58 ± 1.44 *	26.33 ± 1.95
C20:4 n-6 (AA)	314.84 ± 6.38	277.13 ± 2.48	269.37 ± 1.78	338.36 ± 44.67 ¥	317.85 ± 15.25 ¥	203.91 ± 2.73 #	185.39 ± 5.99 *	195.29 ± 13.48
C20:5 n-3 (EPA)	450.26 ± 2.05	400.48 ± 22.37	451.25 ± 13.07	200.83 ± 5.67 ¥	203.16 ± 10.21 ¥	127.58 ± 0.95 #	100.79 ± 8.65 *	114.83 ± 5.05 *
C20:3 n-6	87.23 ± 7.07	84.27 ± 2.34	67.61 ± 0.67	81.62 ± 2.39 ¥	89.69 ±1.34 ¥	65.15 ± 2.24 #	81.93 ± 2.81 *	72.33 ± 3.41 *
C20:2 n-6	52.96 ± 2.27	47.51 ± 0.10	51.64 ± 1.70	32.50 ± 0.25 ¥	36.01 ± 4.04 ¥	15.72 ± 2.19 #	17.71 ± 1.38*	34.50 ± 1.08 *
C22:6 n-3 (DHA)	95.82 ± 2.21	82.47 ± 0.90	79.76 ± 1.66	98.43 ± 5.62 ¥	97.45 ± 4.70 ¥	70.85 ± 0.86 #	70.65 ± 0.46	76.97 ± 3.81 *
C22:5 n-3 (DPA)	92.21 ± 1.70	90.63 ± 3.51	79.05 ± 1.42	93.39 ± 5.68 ¥	89.42 ± 2.41 ¥	63.52 ± 0.87 #	76.81 ± 0.17 *	75.06 ± 0.15 *
∑PUFA	1588.33 ± 14.33	1373.67 ± 29.60	1512.94 ± 4.59	1318.22 ± 34.65 ¥	870.35 ± 39.09 ¥	872.40 ± 22.61 #	562.57 ± 0.47 *	628.02 ± 1.89 *
∑PUFA (n-3)	638.29 ± 5.97	573.58 ± 26.79	610.05 ± 9.99	392.65 ± 5.60 ¥	390.04 ± 17.32 ¥	261.95 ± 0.95 #	248.25 ± 8.02 *	266.85 ± 8.71
∑PUFA (n-6)	487.70 ± 5.07	436.96 ± 1.18	418.35 ± 1.16	488.78 ± 43.66 ¥	480.31 ± 21.77 ¥	307.91 ± 4.25 #	311.61 ± 6.01	328.45 ± 17.76
∑PUFA n-3/∑PUFA n-6	1.31 ± 0.00	1.31 ± 0.06	1.46 ± 0.03	0.81 ± 0.06 ¥	0.81 ± 0.00 ¥	0.85 ± 0.01 #	0.80 ± 0.04	0.82 ± 0.07
Δ 4 : C22:6 n-3/C22 :5 n-3	1.04 ± 0.00	0.91 ± 0.03	1.01 ± 0.00	1.06 ± 0.12	1.09 ± 0.02 ¥	1.12 ± 0.03 #	0.92 ± 0.00 *	1.03 ± 0.05 *
Δ 5: C20:4 n-6 /C20:3 n-6	3.64 ± 0.37	3.29 ± 0.12	3.98 ± 0.01	4.16 ± 0.67	3.55 ± 0.22 ¥	3.13 ± 0.07	2.27 ± 0.15 *	2.70 ± 0.06 *
Δ 8: C20:3 n-6 /C20 :2 n-6	1.64 ± 0.06	1.77 ± 0.05	1.31 ± 0.06	2.51 ± 0.09 ¥	2.53 ± 0.32 ¥	4.25 ± 0.73 #	4.67 ± 0.52	2.10 ± 0.16 *
Δ 9: C16:1 n-7/ C16:0	0.19 ± 0.01	0.18 ± 0.02	0.16 ± 0.00	0.21 ± 0.00 ¥	0.24 ± 0.00 ¥	0.18 ± 0.00	0.23 ± 0.00 *	0.21 ± 0.00 *
Δ 9: C18:1 n-9/ c18:0	1.81 ± 0.02	1.74 ± 0.07	1.92 ± 0.05	2.35 ± 0.01 ¥	1.86 ± 0.02	2.73 ± 0.01 #	2.17 ± 0.02 *	2.12 ± 0.01 *
Elongase: 22:5 n-3 /C20:5 n-3	0.20 ± 0.00	0.23 ± 0.00	0.18 ± 0.01	0.47 ± 0.04 ¥	0.44 ± 0.01 ¥	0.50 ± 0.00 #	0.77 ± 0.07 *	0.65 ± 0.03 *
Elongase : C18:0/C16:0	0.53 ± 0.00	0.51 ± 0.02	0.42 ± 0.01	0.45 ± 0.02 ¥	0.58 ± 0.01 ¥	0.42 ± 0.02 #	0.49 ± 0.00 *	0.32 ± 0.00 *

*Concentrations are expressed as ng/million cells. Results are expressed as mean ± SD of three independent experiments. A two way ANOVA followed by a Student's t-test was realized. Significant difference between vehicle (EtOH 0.6%) and 7β-OHC-treated cells is indicated by **#**; P < 0.05; significant difference between 7β-OHC and (7β-OHC + DMF) or (7β-OHC + MMF) is indicated by *; P < 0.05; significant difference between vehicle (DMSO 0.05%) and DMF or MMF treated cells is indicated by ¥; P < 0.05. No significant differences are observed between Control, EtOH and DMSO. **∑PUFA:** sum of polyunsaturated fatty acids; **Δ 4:** delta 4 desaturase**; Δ 5:** delta 5 desaturase; **Δ 8:** delta 8 desaturase; **Δ 9:** delta 9 desaturase; 7β-hydroxycholesterol: 7β-OHC.*

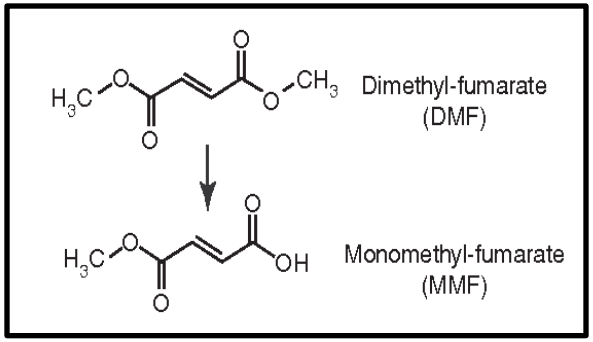

Neuroprotective properties of DMF and MMF (158N oligodendrocytes)

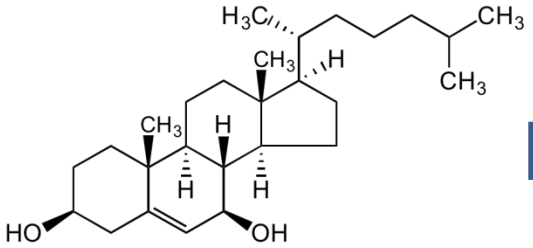

7β-hydroxycholesterol

Oxiapoptophagy

- *Oxidative stress*
- *Mitochondrial dysfunctions / apoptosis*
- *Autophagy*

Modifications of lipid profile
(sterols, fatty acids)

SGHAIER R et al. Graphical Abstract